Supplementary Information (SI) for Physical Chemistry Chemical Physics.

Supplementary Information: Inferring Networks of Chemical Reactions by Curvature Analysis of Kinetic Trajectories

Vignesh Narayanan,[†] Lawrence K. Bordoh,[‡] István Z. Kiss,[*,‡] and Jr-Shin Li[¶]

†*AI Institute, University of South Carolina, 1112 Greene St, Columbia, SC 29208.*

‡*Department of Chemistry, Saint Louis University, 3501 Laclede Ave, St. Louis, MO 63103.*

¶*Department of Electrical and Systems Engineering, Washington University in St. Louis, 1 Brookings Dr, St. Louis, MO 63130*

E-mail: istvan.kiss@slu.edu

This supplementary document is organized as follows:

- Section 1 includes the proposed perturbation method for a general case.
- Section 2 contains details of experimental methods used to obtain results with electrochemical networks.
- Section 3 includes all the experimental results and the associated data plots.

1 Perturbation strategy for inferring coupling

The dynamics of agent k following a perturbation (or control) input is given by

$$\dot{x}_k^{(e)}(t) = f(x_k^{(e)}) + g_k(x_k^{(e)})u_k^{(e)}(t) + \sum_{j=1, j\neq k}^{N} K_{kj}(x_j^{(e)} - x_k^{(e)}), \tag{1}$$

where $u_k^{(e)}$ is the control input to agent k, $x_k^{(e)}$ is an n-dimensional state vector respectively, and $\dot{x}_k^{(e)}$ is the resulting dynamics during the e^{th} experiment, and $g_k(x_k^{(e)}) \in \mathbb{R}^n$ is a nonlinear function modeling the input channel through which $u_k^{(e)}$ affects the dynamics of agent k. Here K_{ij} is the coupling strength between node i and j, modeling the directional connection from node j to node i. Note that for ease of exposition, we set $u_k^{(e)} \in \mathbb{R}$ (single source of actuation at agent k) for each $k = 1, \dots, N$, and from hereon, we drop the superscript (e) from the state trajectories of all the agents during the e^{th} experiment and only use it with the perturbation inputs and the response dynamics. We propose a set of short-duration perturbation experiments ($e = 0, 1, \dots, E$) at each agent of the NDN, and, in the following, show that the disparity in the response of the agents to different controls contain the required information to disentangle the natural timescale of a system from its coupling dynamics.

[a] *AI Institute, University of South Carolina, 1112 Greene St, Columbia, SC 29208.*
[b] *Department of Chemistry, Saint Louis University, 3501 Laclede Ave, St. Louis, MO 63103.*
[c] *Department of Electrical and Systems Engineering, Washington University in St. Louis, 1 Brookings Dr, St. Louis, MO 63130. E-mail: istvan.kiss@slu.edu.*
[*] *Corresponding author.*
† Supplementary information available: [details of any supplementary information available should be included here]. See DOI: 00.0000/00000000.
‡These authors contributed equally to this work.

Let $\Delta_e u_k(t) = u_k^{(0)}(t) - u_k^{(e)}(t)$ and $\Delta_e \dot{x}_k(t, a_{k0}) = \dot{x}_k^{(0)}(t) - \dot{x}_k^{(e)}(t)$ denote the difference between the control applied at the reference (the zeroth) and the e^{th} experiment and the difference between the resulting dynamics with the same initial condition, i.e., $x_k^{(0)}(t_0) = x_k^{(e)}(t_0) = a_{k0}$ for $k = 1, \ldots, N$, respectively. Then, from (1), we obtain

$$\Delta_e \dot{x}_k(t_0, a_{k0}) = g_k(a_{k0}) \Delta_e u_k(t_0), \tag{2}$$

with $\Delta_e x_k(t_0) = 0$ for $e = 1, \ldots, E$. This informs that the effect of the input channel, i.e., the state-dependent control coefficient g_k at a_{k0}, on the control can be estimated by observing the variations in the controls and the resultant dynamics of x_k at the sample point a_{k0}. Note that the computation of the variation in the dynamics to different perturbations helps cancel the effect of the drift at the sample point a_{k0}, and hence, aids in isolating the unknown nonlinear function g_k from the drift and the coupling functions.

Motivated by this observation, to separate the coupling functions from the drift of agent k, we utilize the response of the other agents in the NDN to the perturbation inputs applied at agent k. In particular, the dynamics of agent i ($i \neq k$) following (1) in the absence of controls ($u_i^{(e)}(t) = 0$) with the initial conditions $x_i^{(e)}(t_0) = a_{i0}$ is given by $\dot{x}_i^{(e)}(t) = f(x_i) + \sum_{j=1, j\neq i}^{N} K_{ij}(x_j - x_i)$. Since the effect of the perturbation applied to agent k on the dynamics of agent i is only indirect, the information about the coupling functions is encoded in the "curvature" or the second-order time-derivative of the state of agent i. In fact, if the initial condition of the NDN for each experiment is fixed, then the difference in the rates of agent k between the reference perturbation experiment and the e^{th} experiment ($\Delta_e \dot{x}_k$), and the corresponding difference in the curvatures of the state of agent i (i.e., $\Delta_e \ddot{x}_i$) are proportional. In particular, their relation is given by

$$\Delta_e \ddot{x}_i(t_0, a_{i0}) = K_{ik} \Delta_e \dot{x}_k(t_0, a_{k0}), \tag{3}$$

where $\Delta_e \ddot{x}_i(t, a_{i0}) = \ddot{x}_i^{(0)}(t) - \ddot{x}_i^{(e)}(t)$ with $e = 1, \ldots, E$. This reveals that the forced measurement data obtained from these perturbation experiments contain sufficient information to infer the value of K_{ik} for $i = 1, \dots, N$ and $i \neq k$.

Note that the equations derived in (3) is independent of the drift f or the control coefficients g_k, i.e., local dynamics. We can utilize these systems of linear equations for each node along with the stimulated data from the perturbation experiments for recovering K_{ik} for each $i, k = 1, \dots, N$ and $i \neq k$. Furthermore, the recovered K_{ik} for each $i, k = 1, \dots, N$, can be utilized together with the data to infer the drift-dynamics f of the agents.

2 Numerical example

In this example, we consider a network of 3 Lorenz oscillators governed by the dynamic equations

$$\begin{aligned}
\dot{x}_i(t) &= \sigma(y_i(t) - x_i(t)) + \sum_{i,j=1, j\neq i}^{3} c_{ij} x_j(t) \\
\dot{y}_i(t) &= r x_i(t) - y_i(t) - x_i(t) z_i(t) + \sum_{i,j=1, j\neq i}^{3} d_{ij} y_j(t) \\
\dot{z}_i(t) &= -b z_i(t) + x_i(t) y_i(t).
\end{aligned} \tag{4}$$

The oscillator network has both x and y couplings. We consider inferring the network topology corresponding to the y couplings, and in particular, estimate d_{ij} for each i, j. To do this task, we require that we are able to perturb the dynamics of y_i for $i = 1, 2, 3$ using any controllable parameter and have access to measurement data for the variables $y_i(t)$. For instance, we consider an external control parameter for the dynamics of y_i, resulting in the dynamics

$$\dot{x}_i(t) = \sigma(y_i(t) - x_i(t)) + \sum_{i,j=1,j\neq i}^{3} c_{ij}x_j(t)$$

$$\dot{y}_i(t) = rx_i(t) - y_i(t) - x_i(t)z_i(t) + \sum_{i,j=1,j\neq i}^{3} d_{ij}y_j(t) + u_i(t)$$

$$\dot{z}_i(t) = -bz_i(t) + x_i(t)y_i(t), \tag{5}$$

where u_i for $i = 1, 2, 3$ are external controls. For illustration, we consider multiple cases.

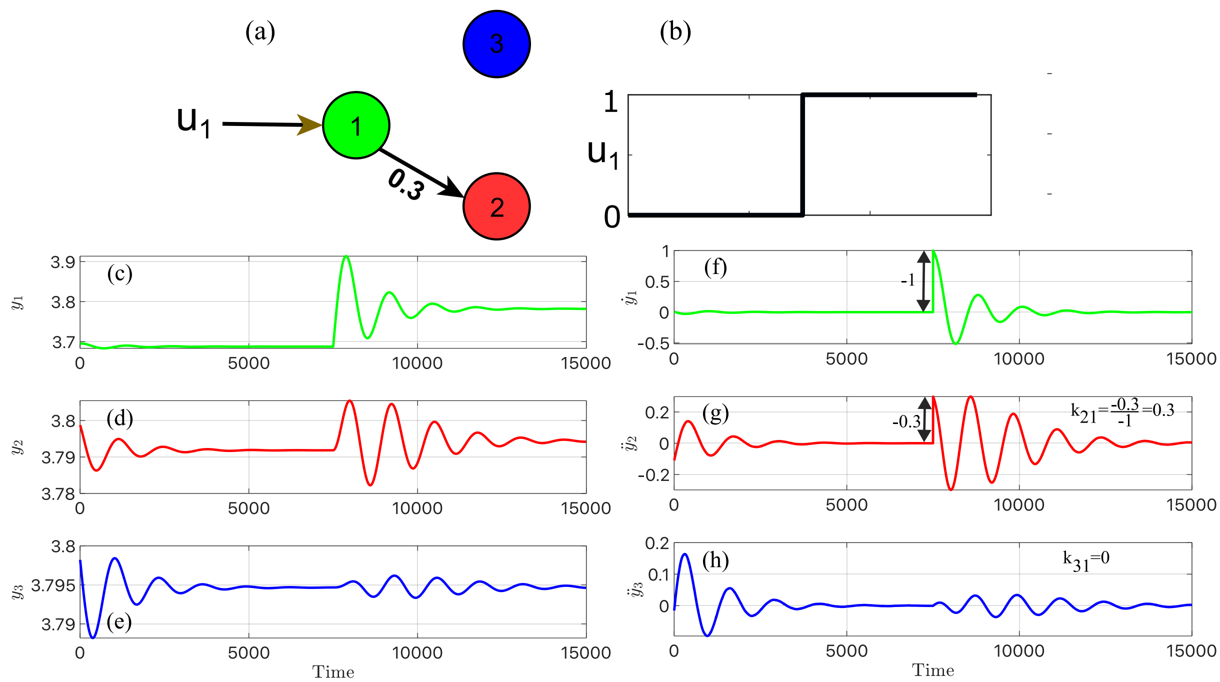

Figure 1 (a) A three node (directed chain) network of damped Lorenz systems with directed y -coupling. Perturbation u_1 is applied to node 1 to infer its outgoing connections. (b) The step input applied at node 1 at time t = 7500ms. (c)-(e) Time series data of variable y at nodes 1,2, and 3. (f) The slope $\dot{y}_1(t)$ computed at node 1 using Euler approximation. (g)-(h) The curvature $\ddot{y}_i(t)$ for $i = 2, 3$ computed at nodes 2 and 3 using Euler approximation. The ratio of the curvature of the coupled nodes ($\ddot{y}_i$, $i = 2, 3$) with respect to the slope of the perturbed node $\dot{y}_1$ at the time of application of the step input ($t_0 = 7500$ms) reveals the outgoing connections of node 1.

- Case 1: The parameters in (5) are set as follows: $\sigma = 10, r = 6.1, b = \frac{8}{3}$. Here the Lorenz system has a stable attractor. We consider three Lorenz systems governed by (5) with the initial conditions set at $(1, 0.3, 0.1), (1, 0.3, 0.2), (1, 0.9, 0.8)$ for each experiment. The number of simulations e at each node was set as $E = 2$. We apply a unit step input at $t = t_0$, with $t_0 = 7500$ms. The perturbation signals were selected as $u_i^{(0)}(t) = 0$ and $u_i^{(1)}(t) = \left\{ \begin{smallmatrix} 0 & t<t_0 \\ 1 & t\geq t0 \end{smallmatrix} \right.$. A total of six experiments were conducted, (applying the two perturbation signals at each node). The coupling strengths, d_{ij} was selected as follows: $d_{12} = d_{23} = 0.3$ and rest of the coupling strengths were set as zero. In the first two experiments, the u_1 was used to perturb the node 1. The ini-

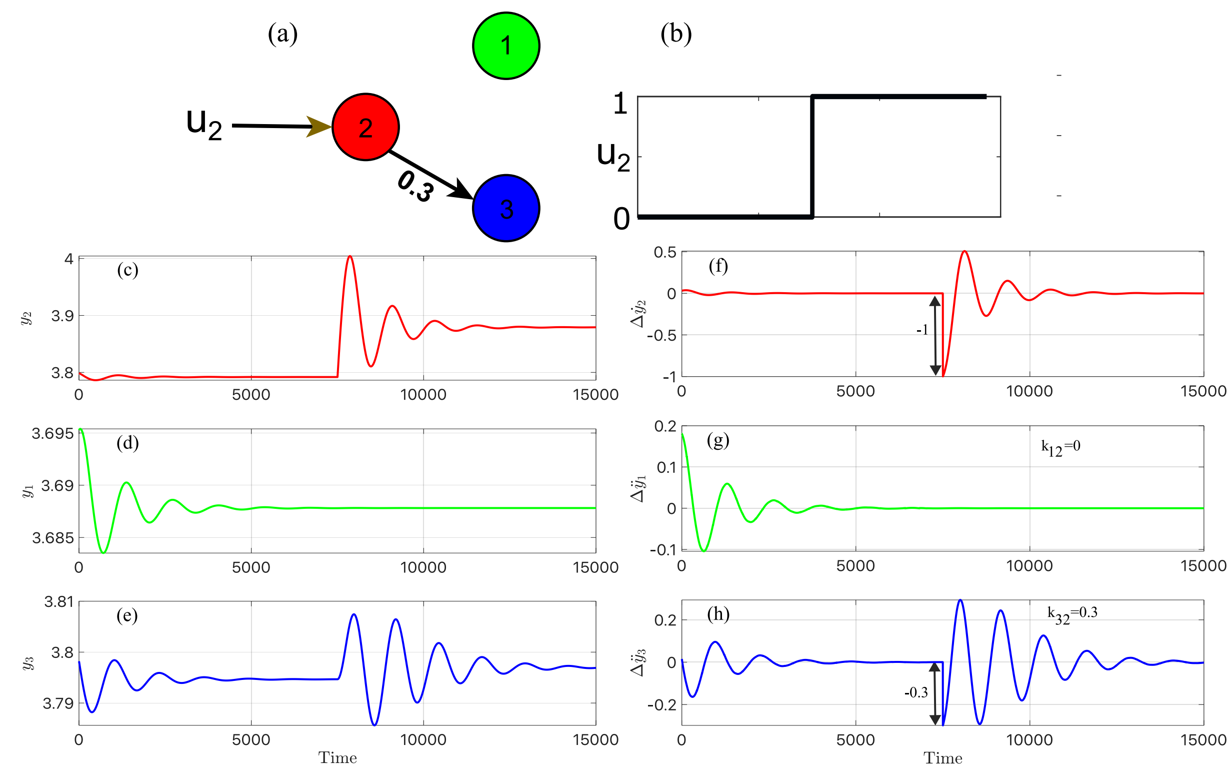

Figure 2 (a) Perturbation u_2 is applied to node 2 to infer its outgoing connections. (b) The step input applied at node 2 at time $t = 7500$ms. (c)-(e) Time series data of variable y at nodes 1,2, and 3. (f) The slope $\dot{y}_2(t)$ computed at node 1 using Euler approximation. (g)-(h) The curvature $\ddot{y}_i(t)$ for $i = 1, 3$ computed at nodes 1 and 3 using Euler approximation. The ratio of the curvature of the coupled nodes ($\ddot{y}_i$, $i = 1, 3$) with respect to the slope of the perturbed node $\dot{y}_2$ at the time of application of the step input ($t_0 = 7500$ms) reveals the outgoing connections of node 2.

tial conditions were unchanged in both the experiments (i.e., $x(t_0), y(t_0), z(t_0)$ were fixed). Computing the difference in the second derivatives for the two simulations yields the following linear equations

$$\begin{aligned}
&\Delta_1\ddot{y}_2(t_0) = d_{21}\Delta_1\dot{y}_1(t_0), \quad \Delta_1 y_2(t_0) = 0, \quad \Delta_1\dot{y}_2(t_0) = 0, \\
&\Delta_1\ddot{y}_3(t_0) = d_{31}\Delta_1\dot{y}_1(t_0), \quad \Delta_1 y_3(t_0) = 0, \quad \Delta_1\dot{y}_3(t_0) = 0.
\end{aligned} \tag{6}$$

Using $\Delta_1\ddot{y}_2(t_0)$, $\Delta_1\ddot{y}_3(t_0)$, and $\Delta_1\dot{y}_1(t_0)$, the coupling strengths d_{21} and d_{31} were recovered. Similarly, the second pair of experiments involved applying step signal u_2 to perturb node 2, and the last pair of experiments were performed by varying u_3 at node 3. The simulated trajectories are shown in Figures 1-3.

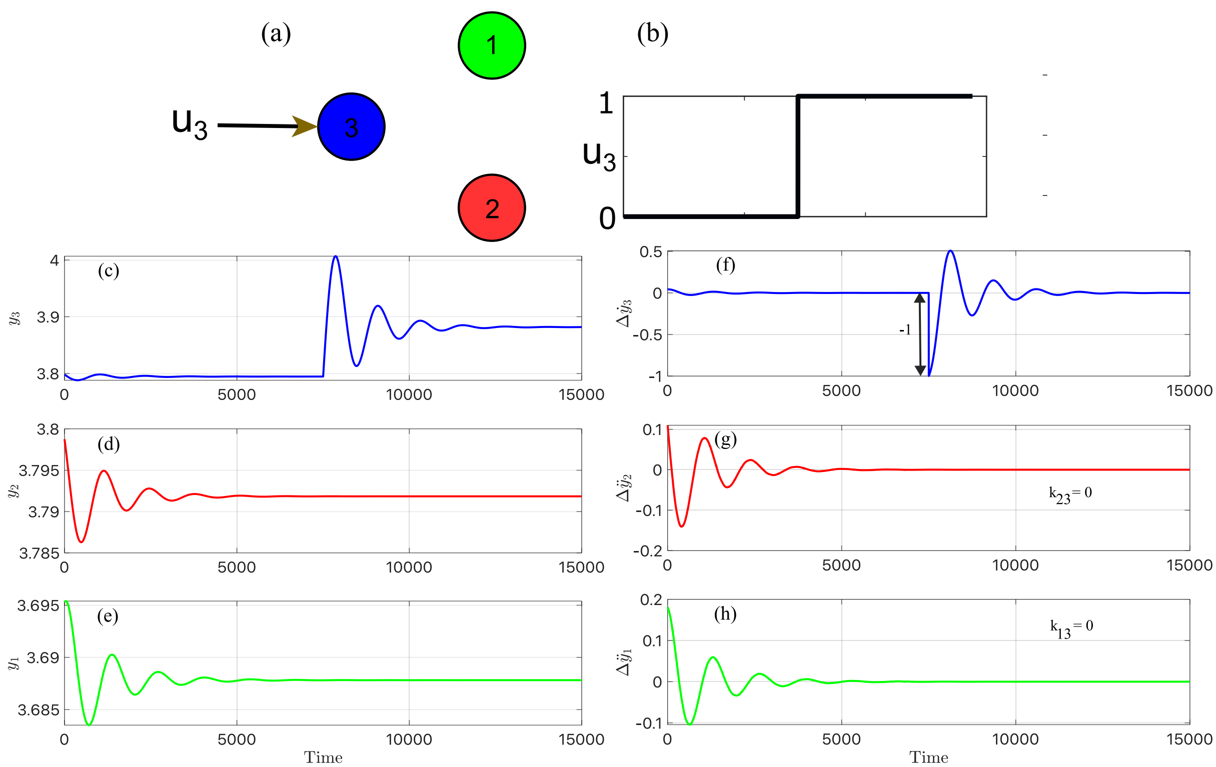

Figure 3 (a) Perturbation u_3 is applied to node 3 to infer its outgoing connections. (b) The step input applied at node 3 at time $t = 7500$ms. (c)-(e) Time series data of variable y at nodes 1,2, and 3. (f) The slope $\dot{y}_3(t)$ computed at node 1 using Euler approximation. (g)-(h) The curvature $\ddot{y}_i(t)$ for $i = 1, 2$ computed at nodes 1 and 2 using Euler approximation. The ratio of the curvature of the coupled nodes ($\ddot{y}_i$, $i = 1, 2$) with respect to the slope of the perturbed node $\dot{y}_3$ at the time of application of the step input ($t_0 = 7500$ms) reveals the outgoing connections of node 3.

- Case 2: Here we set the parameters of all the three Lorenz system (5) as follows:

$\sigma = 10, r = 28, b = \frac{8}{3}$. The initial conditions were same as case 1. In this case, the dynamics of the Lorenz system were operating within the chaotic regime.

We apply a step input at $t = t_0$, with $t_0 = 7500$ms and step size 10. The perturbation signals were selected as $u_i^{(0)}(t) = 0$ and $u_i^{(1)}(t) = \left\{ \begin{smallmatrix} 0 & t<t_0 \\ 10 & t\geq t0 \end{smallmatrix} \right.$. A total of six experiments were conducted, (applying the two perturbation signals at each node). The coupling strengths, d_{ij} was selected as follows: $d_{12} = d_{23} = 0.3$ and rest of the coupling strengths were set as zero. The simulated trajectories are shown in Figures 4-6.

- Case 3: Here we illustrate our curvature analysis by applying perturbations through the parameter r_i in (4). The initial conditions and parameters were selected to be similar to those in case 2. We conducted six experiments by perturbing the parameter r_i at each node. In the first experiment at node i, r_i was set to 28, while in the second experiment, r_i was perturbed and set to 32. The value of r_i, $j \neq i$ were left unchanged for both experiments. The simulated trajectories are shown in Figures 7-9.

- Case 4: Here we illustrate our curvature analysis by applying perturbations through an external input u_i for a 7-node network of Lorenz systems. The parameters for all the nodes were selected to be similar to those in the Case 1. Perturbation was applied to each individual node in the network and the evolution of the signal of the various node analyzed. The network topology and the step perturbation applied to node 1 for inferring the outgoing connections of node 1 are shown in Figure 10. The resulting y-trajectories for all the seven nodes are shown in Figure 11. The computed slope of y_1 and the curvatures of $y_2, y_3, \ldots, y_7$ are shown in Figure 12. For the purpose of illustration, we record the results only for the two experiments conducted at node 1, resulting in correctly recovering the coupling strengths of the outgoing connections of node 1.

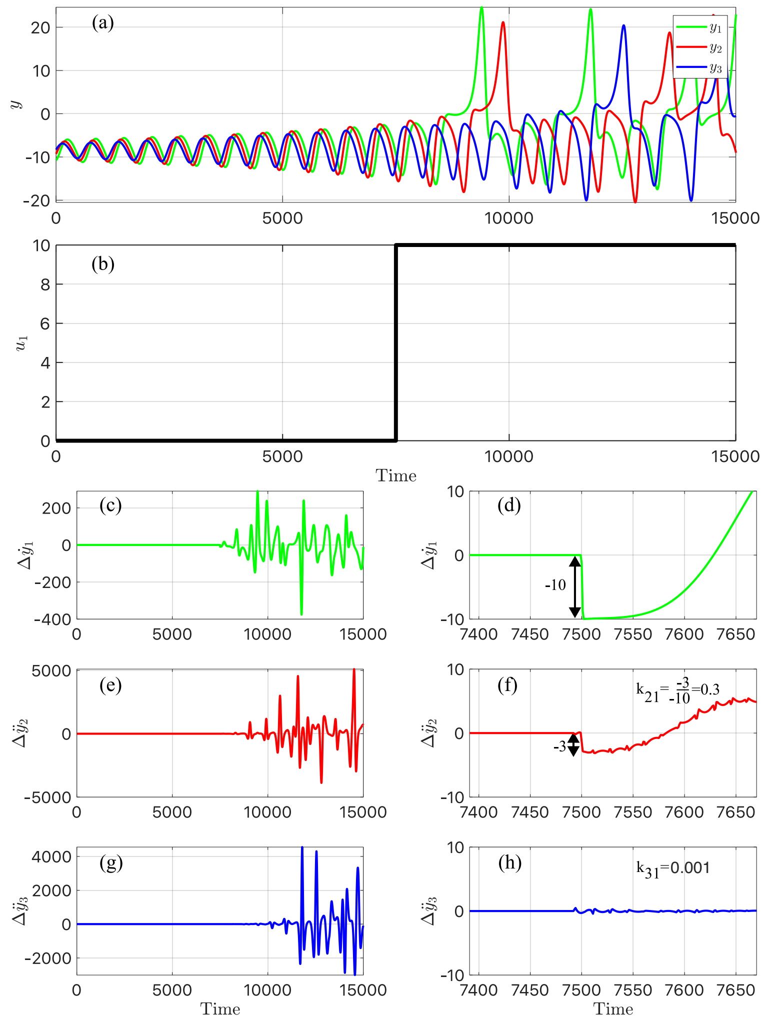

Figure 4 (a) The y trajectories of all the three Lorenz system showing chaotic evolution. (b) The step perturbation applied at node 1 at time $t = 7500$ms through the external control parameter u_1 to infer its outgoing connections. (c) The change in slope $\Delta\dot{y}_1(t)$ computed at node 1 using Euler approximation. (d) The change in slope $\Delta\dot{y}_1(t)$ zoomed in around $t = t_0$. (e)(g) The curvature change $\Delta\ddot{y}_i(t)$ for $i = 2, 3$ computed at nodes 2 and 3 using Euler approximation. (f)(h) The curvature change zoomed in at $t = t_0$ of the coupled nodes ($\Delta\ddot{y}_i$, $i = 2, 3$). The ratio of the curvature of the coupled nodes ($\Delta\ddot{y}_i$, $i = 2, 3$) with respect to the slope of the perturbed node $\Delta\dot{y}_1$ at the time of application of the step input ($t_0 = 7500$ms) reveals the outgoing connections of node 1.

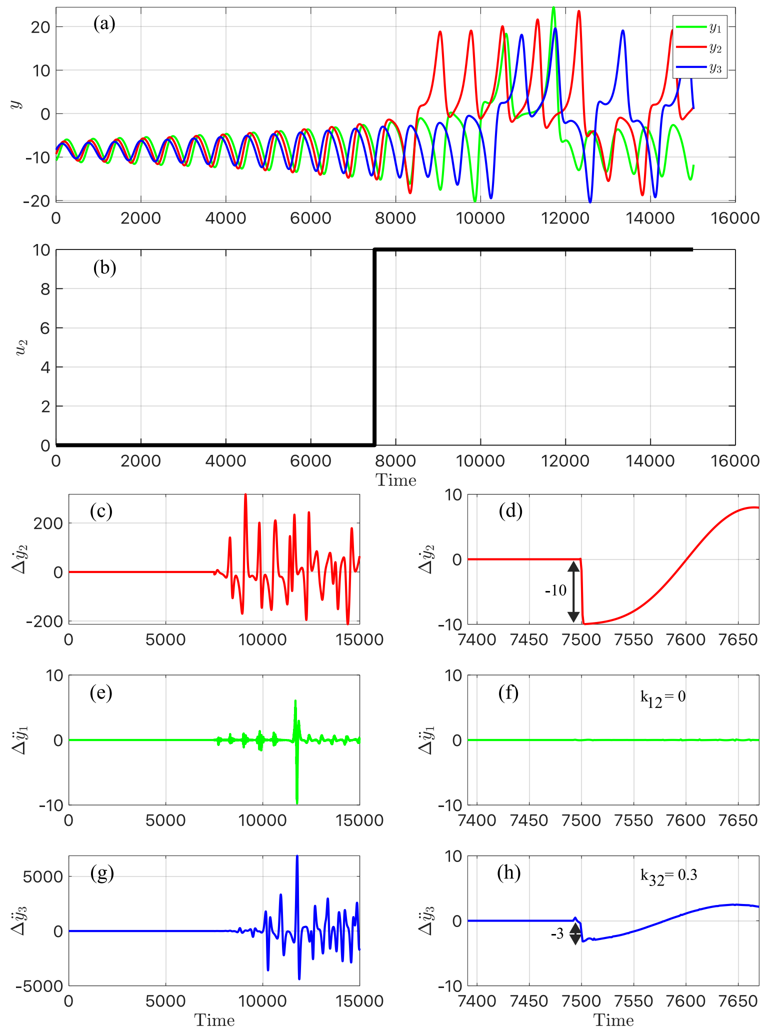

Figure 5 (a) The y trajectories of all the three Lorenz system showing chaotic evolution. (b) The step perturbation applied at node 2 at time $t = 7500$ms through the external control parameter u_2 to infer its outgoing connections. (c) The change in slope $\Delta\dot{y}_2(t)$ computed at node 2 using Euler approximation. (d) The change in slope $\Delta\dot{y}_2(t)$ zoomed in around $t = t_0$. (e)(g) The curvature change $\Delta\ddot{y}_i(t)$ for $i = 1, 3$ computed at nodes 1 and 3 using Euler approximation. (f)(h) The curvature change zoomed in at $t = t_0$ of the coupled nodes ($\Delta\ddot{y}_i$, $i = 1, 3$). The ratio of the curvature of the coupled nodes ($\Delta\ddot{y}_i$, $i = 1, 3$) with respect to the slope of the perturbed node $\Delta\dot{y}_2$ at the time of application of the step input ($t_0 = 7500$ms) reveals the outgoing connections of node 2.

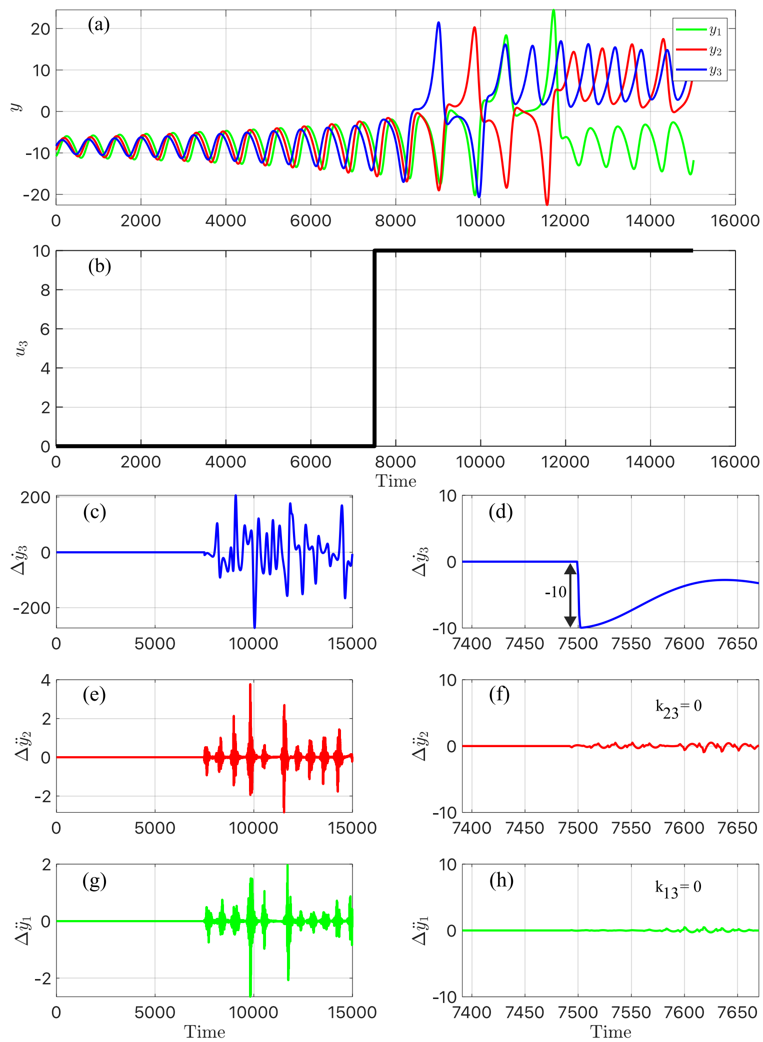

Figure 6 (a) The y trajectories of all the three Lorenz system showing chaotic evolution. (b) The step perturbation applied at node 3 at time $t = 7500$ms through the external control parameter u_3 to infer its outgoing connections. (c) The change in slope $\Delta\dot{y}_3(t)$ computed at node 3 using Euler approximation. (d) The change in slope $\Delta\dot{y}_3(t)$ zoomed in around $t = t_0$. (e)(g) The curvature change $\Delta\ddot{y}_i(t)$ for $i = 1, 2$ computed at nodes 1 and 2 using Euler approximation. (f)(h) The curvature change zoomed in at $t = t_0$ of the coupled nodes ($\Delta\ddot{y}_i$, $i = 1, 2$). The ratio of the curvature of the coupled nodes ($\Delta\ddot{y}_i$, $i = 1, 2$) with respect to the slope of the perturbed node $\Delta\dot{y}_3$ at the time of application of the step input ($t_0 = 7500$ms) reveals the outgoing connections of node 3.

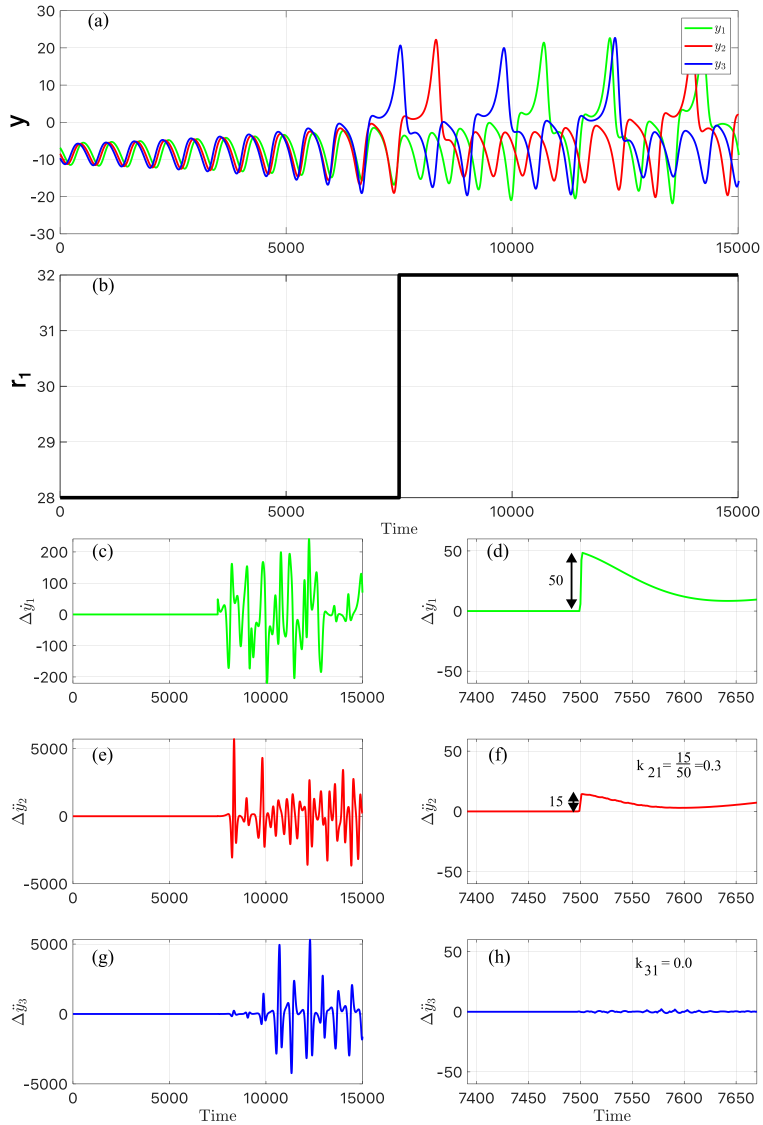

Figure 7 (a) The y trajectories of all the three Lorenz system showing chaotic evolution. (b) The step perturbation applied at node 2 at time $t = 7500$ms through the parameter r_1 to infer its outgoing connections. (c) The change in slope $\Delta\dot{y}_1(t)$ computed at node 1 using Euler approximation. (d) The change in slope $\Delta\dot{y}_1(t)$ zoomed in around $t = t_0$. (e)-(g) The curvature change $\Delta\ddot{y}_i(t)$ for $i = 2, 3$ computed at nodes 2 and 3 using Euler approximation. (f)(h) The curvature change zoomed in at $t = t_0$ of the coupled nodes ($\Delta\ddot{y}_i$, $i = 2, 3$). The ratio of the curvature of the coupled nodes ($\Delta\ddot{y}_i$, $i = 2, 3$) with respect to the slope of the perturbed node $\Delta\dot{y}_1$ at the time of application of the step input ($t_0 = 7500$ms) reveals the outgoing connections of node 1.

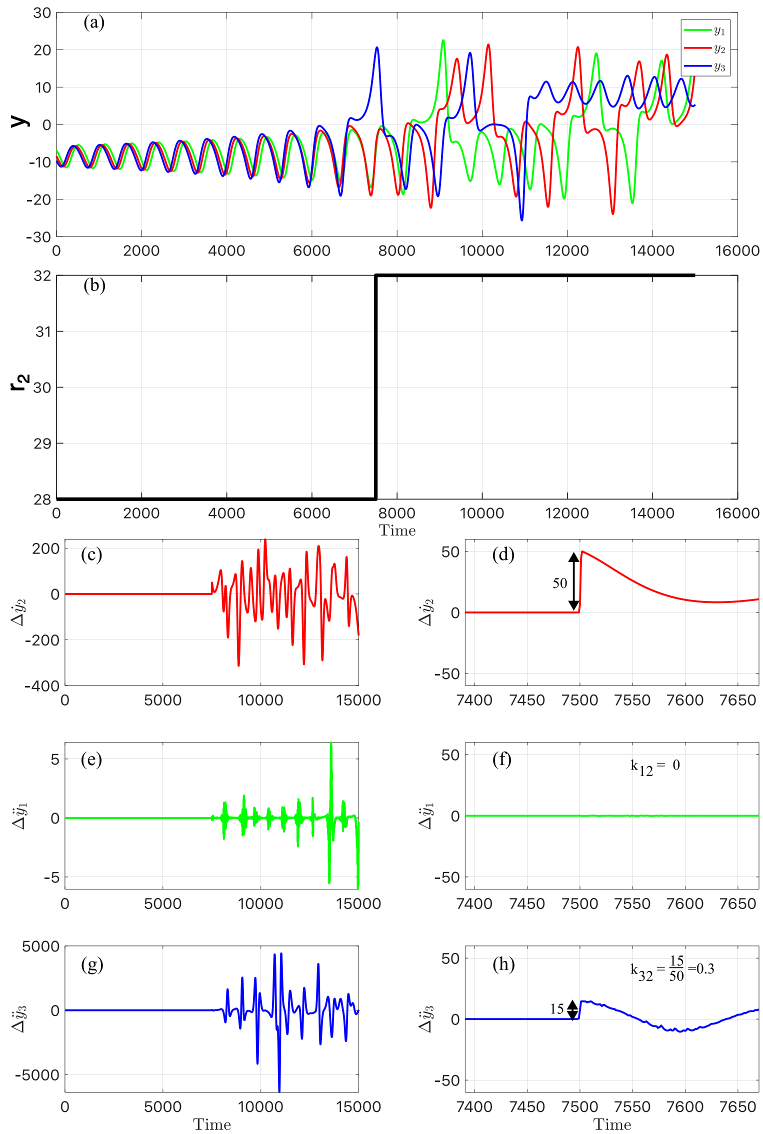

Figure 8 (a) The y trajectories of all the three Lorenz system showing chaotic evolution. (b) The step perturbation applied at node 2 at time $t = 7500\text{ms}$ through the parameter r_2 to infer its outgoing connections. (c) The change in slope $\Delta\dot{y}_2(t)$ computed at node 2 using Euler approximation. (d) The change in slope $\Delta\dot{y}_2(t)$ zoomed in around $t = t_0$. (e)(g) The curvature change $\Delta\ddot{y}_i(t)$ for $i = 1, 3$ computed at nodes 1 and 3 using Euler approximation. (f)(h) The curvature change zoomed in at $t = t_0$ of the coupled nodes ($\Delta\ddot{y}_i$, $i = 1, 3$). The ratio of the curvature of the coupled nodes ($\Delta\ddot{y}_i$, $i = 1, 3$) with respect to the slope of the perturbed node $\Delta\dot{y}_2$ at the time of application of the step input ($t_0 = 7500\text{ms}$) reveals the outgoing connections of node 2.

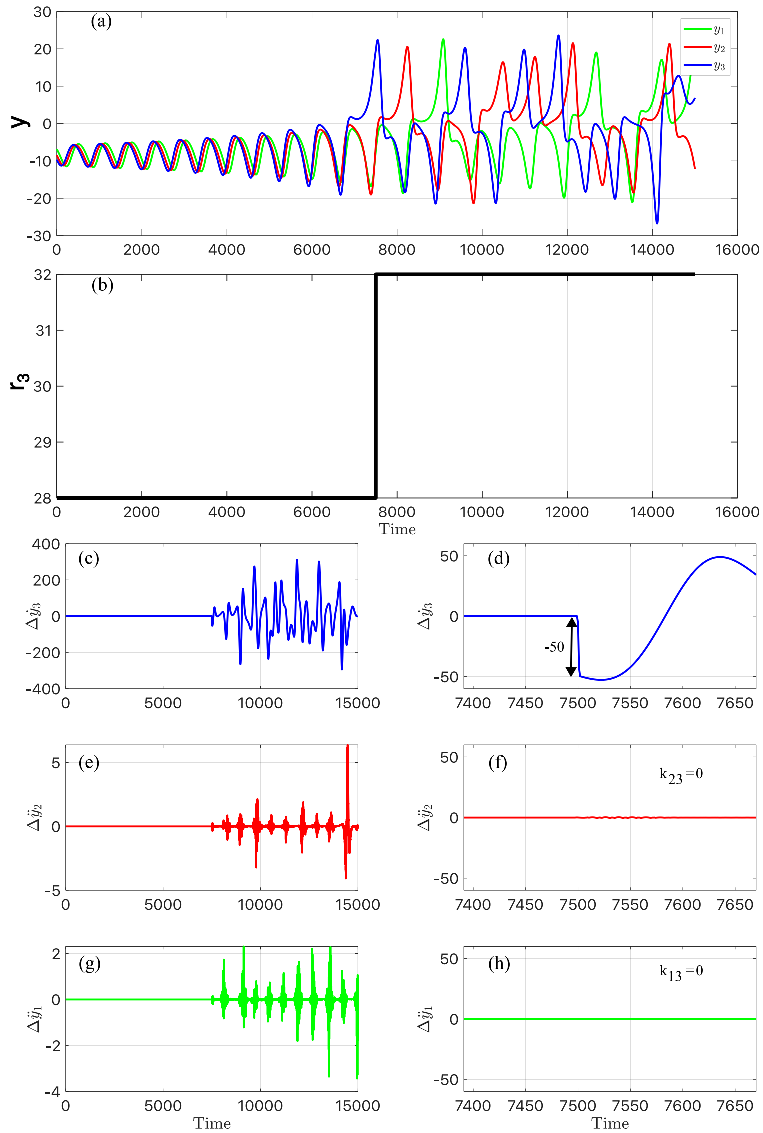

Figure 9 (a) The y trajectories of all the three Lorenz system showing chaotic evolution. (b) The step perturbation applied at node 3 at time $t = 7500$ms through the parameter r_3 to infer its outgoing connections. (c) The change in slope $\Delta\dot{y}_3(t)$ computed at node 3 using Euler approximation. (d) The change in slope $\Delta\dot{y}_3(t)$ zoomed in around $t = t_0$. (e)(g) The curvature change $\Delta\ddot{y}_i(t)$ for $i = 1, 2$ computed at nodes 1 and 2 using Euler approximation. (f)(h) The curvature change zoomed in at $t = t_0$ of the coupled nodes ($\Delta\ddot{y}_i$, $i = 1, 2$). The ratio of the curvature of the coupled nodes ($\Delta\ddot{y}_i$, $i = 1, 2$) with respect to the slope of the perturbed node $\Delta\dot{y}_3$ at the time of application of the step input ($t_0 = 7500$ms) reveals the outgoing connections of node 3.

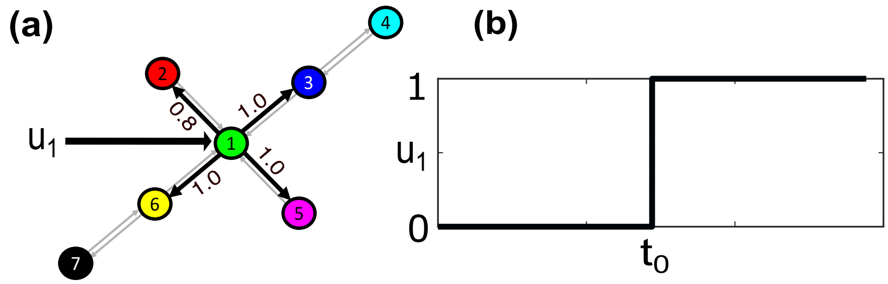

Figure 10 (a) A seven node network of Lorenz systems with directed y -coupling demonstrating damped oscillations. Perturbation u_1 is applied to node 1 to infer its outgoing connections. (b) The step perturbation applied at node 1 at time $t = t_0 = 7500$ms.

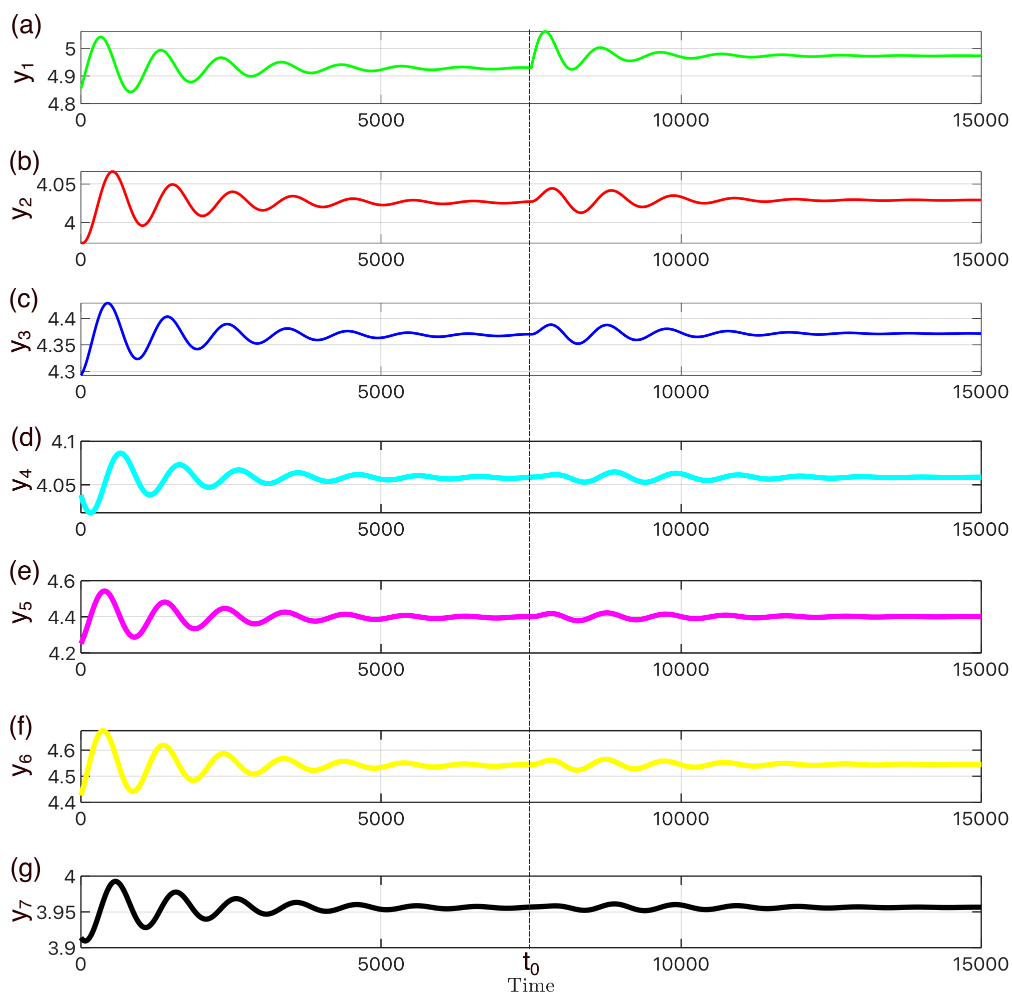

Figure 11 (a)-(g) The y-trajectories of all the seven Lorenz systems for the case when a unit step perturbation was introduced at node 1 at $t = t_0 = 7500$ms.

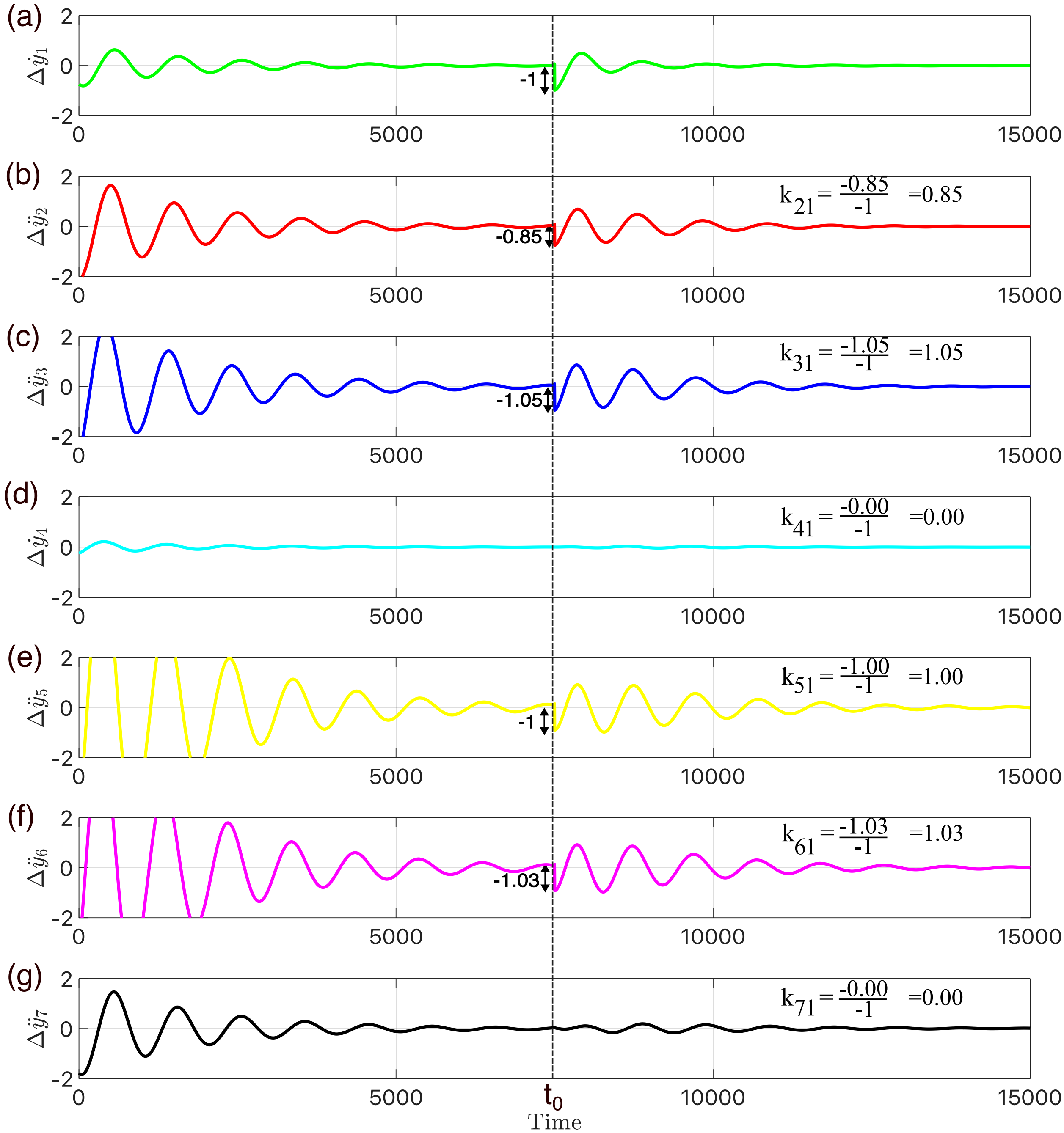

Figure 12 (a) The change in slope of y_1 between the two experiments, i.e., $\Delta\dot{y}_1(t) = \dot{y}_1^0(t) - \dot{y}_1^1(t)$, where for $e = 0$, $u_1(t) = 0$ and for $e = 1$, $u_1(t) = \left\{\begin{smallmatrix} 0 & t<t_0 \\ 1 & t\geq t_0 \end{smallmatrix}\right.$. (b)-(g) The curvature change of y_i for $i = 2, \ldots, 7$ are recorded. It can be observed that at $t_0 = 7500$ms, the curvature change is nontrivial for nodes $2, 3, 5, 6$ indicating outgoing connections from node 1 to these nodes. The coupling strengths are directly determined by computing the ratio of the change in curvature at nodes 2-7 to the change in slope at node 1 at $t = t_0$.

3 Extraction of coupling strengths from experimental data

In the following, we develop the fitting functions used in the curvature analysis procedure using the experimental data. To fix ideas, consider the initial value problem (IVP-1) given by

$$\dot{E}_p(t) = -E_p(t) + 1,$$

with $E_p(0) = 0$, $t \geq 0$. The solution to this IVP-1 is $E_p(t) = 1 - \exp(-t)$. Similarly, for the IVP-2 given by

$$\dot{E}_c(t) = -E_c(t) + E_p(t),$$

with $E_c(0) = 0$, $t \geq 0$, the solutions can be obtained as $E_c(t) = 1 - \exp(-t)(1+t)$. Note that the IVP-1 can be viewed as the unit step response of the linear system $\dot{E}_p(t) = -E_p(t) + u_p(t)$ with $u_p(t) = 1$. When this step response is inturn applied as input to another linear system $\dot{E}_c(t) = -E_c(t) + u_c(t)$, we get the IVP-2. Finally, using the solution of IVP-2 as input to another linear system, we end up with the IVP-3 given by

$$\dot{E}_I(t) = -E_I(t) + E_c(t),$$

with $E_I(0) = 0$, $t \geq 0$, the solutions can be obtained as $E_I(t) = 1 - \exp(-t)(1 + t + 0.5t^2)$.

Since our curvature analysis concerns with the short term response of the systems around the time instant when the perturbations are applied, we use the parameterized step response behavior ($E_p(t)$ from IVP-1) as the fitting function for the perturbed node and the parameterized solution to the IVP-3 as the fitting function for the coupled node. From the experimental results in the bottom panel of Fig. S8a, the perturbed element is approximated using the function

$$E_p(\text{t}) = A_p(1 - \exp(-k_p t)). \tag{7}$$

The data from the coupled electrode is approximated using the function

$$E_c(\text{t}) = A_c(1 - \exp(-k_c t)(1 + k_m t)). \tag{8}$$

For a three electrode in a chain as shown in Fig. S9, where electrode 3 is not directly coupled to electrode 1, we use the function

$$E_c(\text{t}) = A_c(1 - \exp(-k_c t)(1 + k_c t + 0.5 k_m t^2)), \tag{9}$$

to approximate the trajectories of the electrodes that are not perturbed (i.e., the coupled electrodes). Akin to the theory of curvature analysis technique, the change of curvature at the coupled node and the change in the perturbed nodes can be computed using the parametric curves as follows:

$$\frac{d^2 E_c}{dt^2}|_{t=t_0} = \triangle \ddot{E}_c(t_0) = A_c k_c^2 - A_c k_m, \tag{10}$$

and

$$\frac{dE_p}{dt}|_{t=t_0} = \triangle \dot{E}_p(t_0) = A_p k_p. \tag{11}$$

The extracted coupling strength (K_f) employed in the analysis of the experimental result given by the equation

$$K_f = \frac{A_c k_c^2 - A_c k_m}{A_p k_p}. \tag{12}$$

From equation (12), we extracted some parameters from which the coupling can be calculated; A_c which is the amplitude of the coupled electrode after perturbation, A_p which is the amplitude of the perturbed electrode after perturbation, k_p which is the timescale factor of the perturbed electrode, k_c which is the timescale factor of the coupled electrode and k_m which is the timescale factor of the indirectly coupled electrode. When $A_c < 3 \times std[E_{c,b}(t)]$, where $E_{c,b}(t)$ is the electrode potential of the coupled unit before perturbation, we concluded that the observed data is too noisy to infer the weak coupling, and thus the coupling strength is zero.

4 Detailed Experimental Results

A. Network reconstruction using two homogeneous electrodes

The coupling topology to be reconstructed for two electrodes with homogeneous local dynamics was set up as shown below. The term homogeneous was defined as the electrodes having the same individual resistance and the same size.

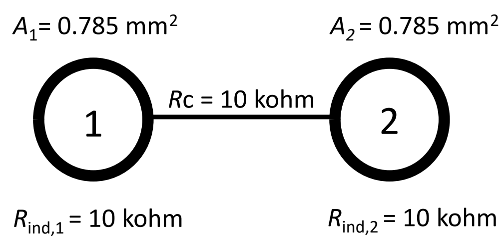

Figure 13 Two electrodes with homogeneous local dynamics.

From the figure above, the applied experimental coupling strength, (κ_{ij}), where i is the coupled electrode and j is the perturbed electrode is given by the equation:

$$\kappa_{ij} = \frac{1}{R_{\text{c}} A_i}$$

where R_{c} is the applied coupling resistance and A_i is the the surface area of the coupled electrode given by the equation

$$A_i = \frac{\pi d^2}{4}$$

where d is the diameter of the electrode which in this case is 1mm.

Table 1 Applied experimental coupling strength for two homogeneous electrodes

$R_{\text{c}}(kohm)$	40	30	20	10	8	6	5	3	2	1	0.8
$\kappa_{ij}(mSmm^{-2})$	0.0318	0.0424	0.0636	0.127	0.159	0.212	0.255	0.424	0.636	1.270	1.590

Table 2 Applied experimental coupling strength $(mSmm^{-2})$ and their corresponding extracted coupling strength (s^{-1}) for two homogeneous electrodes

$\kappa_{ij}(mSmm^{-2})$	0.0318	0.0424	0.0636	0.127	0.159	0.212	0.255	0.424	0.636	1.270	1.590
$A_1(V)$	0.055	0.054	0.053	0.049	0.046	0.044	0.043	0.041	0.038	0.037	0.036
$k1(s^{-1})$	44.68	47.63	45.08	48.66	46.88	49.78	49.78	48.18	50.22	44.73	44.99
$A_2(V)$	0.0053	0.0079	0.0086	0.014	0.015	0.017	0.018	0.022	0.025	0.028	0.029
$k_2(s^{-1})$	39.12	34.50	50.42	50.10	53.80	53.98	57.97	61.84	72.25	80.82	85.50
$k_3(s^{-1})$	0.59	-0.70	-3.12	2.64	-1.53	0.99	-1.98	-1.94	-1.52	0.97	-0.54
$K_f(s^{-1})$	0.00	0.00	0.00	14.72	20.14	22.6	28.27	42.61	68.40	110.5	130.9

Table 3 Extracted coupling strength versus experimental coupling strength (logarithmic data) for two homogeneous electrodes.

$R_c(kohm)$	10	8	6	5	3	2	1	0.8	0.6	0.4	0.2
$\kappa_{ij}(mSmm^{-2})$	0.127	0.159	0.212	0.255	0.424	0.636	1.270	1.590	2.12	3.18	6.36
$log_{10}\kappa_{ij}$	-0.896	-0.799	-0.674	-0.594	-0.373	-0.196	0.104	0.201	0.326	0.502	0.803
$K_f(s^{-1})$	14.72	20.14	22.60	28.27	42.61	68.40	110.5	130.9	137.6	179.5	193.1
$Log_{10}(Kf)$	1.168	1.304	1.354	1.451	1.629	1.835	2.043	2.117	2.138	2.254	2.286

B. Network reconstruction using two heterogeneous electrodes

The perturbation-based technique was also applied to electrodes with heterogeneous local dynamics where the electrodes had different individual resistance but the same size. The coupling topology to be reconstructed for such electrodes was set up as shown below.

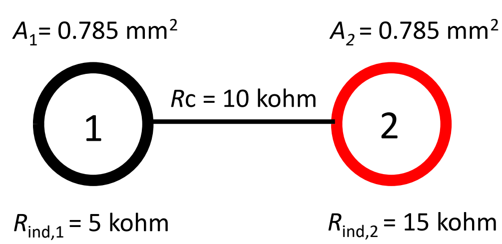

Figure 14 Two electrodes with heterogeneous local dynamics.

Table 4 Extracted coupling strength of two electrodes with heterogeneous dynamics

	Perturbed electrode 1 coupled electrode 2	Perturbed electrode 2 coupled electrode 1
$A_1(V)$	0.0877	0.0524
$k_1(s^{-1})$	241.83	145.69
$A_2(V)$	0.033	0.0117
$k_2(s^{-1})$	184.71	186.159
$k_3(s^{-1})$	1.265	2.533
$K_f(s^{-1})$	53.08	53.10

The effectiveness of the perturbation technique to infer coupling strength between two electrodes with heterogeneous local dynamics, i.e., $R_{\text{ind1}} = 5$ kohm and $R_{\text{ind2}} = 15$ kohm for electrodes 1 and 2 respectively and an applied experimental coupling strength of 0.127 $mSmm^{-2}$, are presented in the table above.

The effect of the parameters that affect directly coupled electrodes (A_p, k_p, A_c, k_c) on the extracted coupling strength for heterogeneous electrodes were examined.

The effect of the amplitudes (α) was described by the following equation:

$$\alpha = [\frac{A_{c,2}/A_{p,2}}{A_{c,1}/A_{p,1}}]$$

where $A_{c,2}$ is the amplitude of coupled electrode 1 when electrode 2 is perturbed. $A_{p,2}$ is the amplitude of perturbed electrode 2 when electrode 2 is perturbed. $A_{c,1}$ is the amplitude of coupled electrode 2 when electrode 1 is perturbed. $A_{p,1}$ is the amplitude of perturbed electrode 1 when electrode 1 is perturbed

From the values of ((A_p, A_c) of the respective perturbations in the table S4 above;

$$\alpha = [\frac{0.0117/0.0524}{0.0330/0.0877}] = \frac{0.59}{1}$$

Thus, the amplitude effect in system is underestimated in the system where electrode 2 is the perturbed node and electrode 1 is the coupled node according to the ratio (0.59:1).

The effect of the timescale (β) was described by the following equation:

$$\beta = [\frac{k_{c,2}/k_{p,2}}{k_{c,1}/k_{p,1}}]$$

where $k_{c,2}$ is the timescale of coupled electrode 1 when electrode 2 is perturbed. $k_{p,2}$ is the timescale of perturbed electrode 2 when electrode 2 is perturbed. $k_{c,1}$ is the timescale of coupled electrode 2 when electrode 1 is perturbed. $k_{p,1}$ is the timescale of perturbed electrode 1 when electrode 1 is perturbed

From the values of ((k_p, k_c) of the respective perturbations in the table S4 above:

$$\beta = [\frac{186.159/145.690}{184.710/241.830}] = \frac{1.67}{1}$$

Thus, the timescale effect in system is overestimated in the system where electrode 2 is the perturbed node and electrode 1 is the coupled node according to the ratio (1.67:1).
The ratio of the coupling strength (γ) was given by the equation:

$$\gamma = \frac{K_{f,2}}{K_{f,1}}$$

where $K_{f,2}$ is the extracted coupling strength when electrode 2 is perturbed. $K_{f,1}$ is the extracted coupling strength when electrode 1 is perturbed.
From the values of K_f of the respective perturbations in the table S4 above;

$$\gamma = \frac{53.10}{53.08} = \frac{1}{1}$$

Thus the estimated coupling strength is the same in the heterogeneous coupled electrodes.

C. Two asymmetric electrodes

The technique was also applied to two asymmetric electrodes to ascertain its robustness and effectiveness. We define asymmetric electrodes as electrodes having different sizes. The figure below shows how the coupling topology was set-up to be reconstructed.

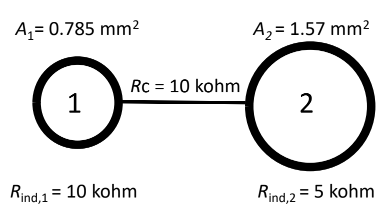

Figure 15 Two asymmetric electrodes .

From the figure above, the estimated extracted coupling strength figures and table for two asymmetric electrodes are shown below.

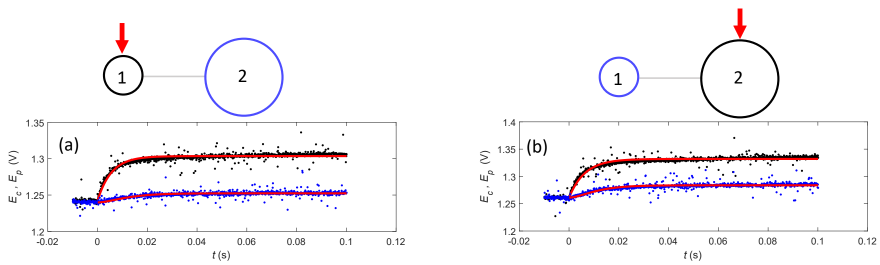

Figure 16 Inference Results for two asymmetric coupled electrodes; (a) Perturbation of electrode 1 (b) Perturbation of electrode2.

Table 5 Extracted coupling strength of two asymmetric electrodes

	Perturbed electrode 1 coupled electrode 2	Perturbed electrode 2 coupled electrode 1
$A_1(V)$	0.0712	0.0615
$k_1(s^{-1})$	157.61	178.48
$A_2(V)$	0.0225	0.0124
$k_2(s^{-1})$	162.96	150.43
$k_3(s^{-1})$	1.783	1.709
$K_f(s^{-1})$	53.24	25.56

Fig S8 denotes the evolution of the signal of the perturbed and coupled electrode. The ratio of the coupling strength (γ) is given by the equation:

$$\gamma = \frac{K_{f,2}}{K_{f,1}}$$

where $K_{f,2}$ is the extracted coupling strength when electrode 2 is perturbed. $K_{f,1}$ is the extracted coupling strength when electrode 1 is perturbed.

From the values of K_f of the respective perturbations in the table S5 above;

$$\gamma = \frac{53.24}{25.56} = \frac{2.08}{1}$$

D. Three electrodes in a linear topology

The coupling topology to be inferred for three electrodes in a chain was setup as shown below.

The extracted coupling strength values and the illustration of the evolution of the signals of three electrodes coupled in a linear topology are shown in Fig S10 and table S6

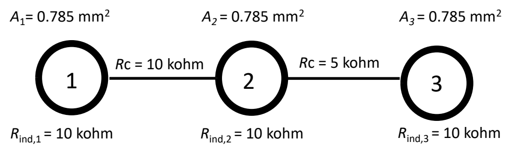

Figure 17 Three electrodes in a chain.

---

respectively.

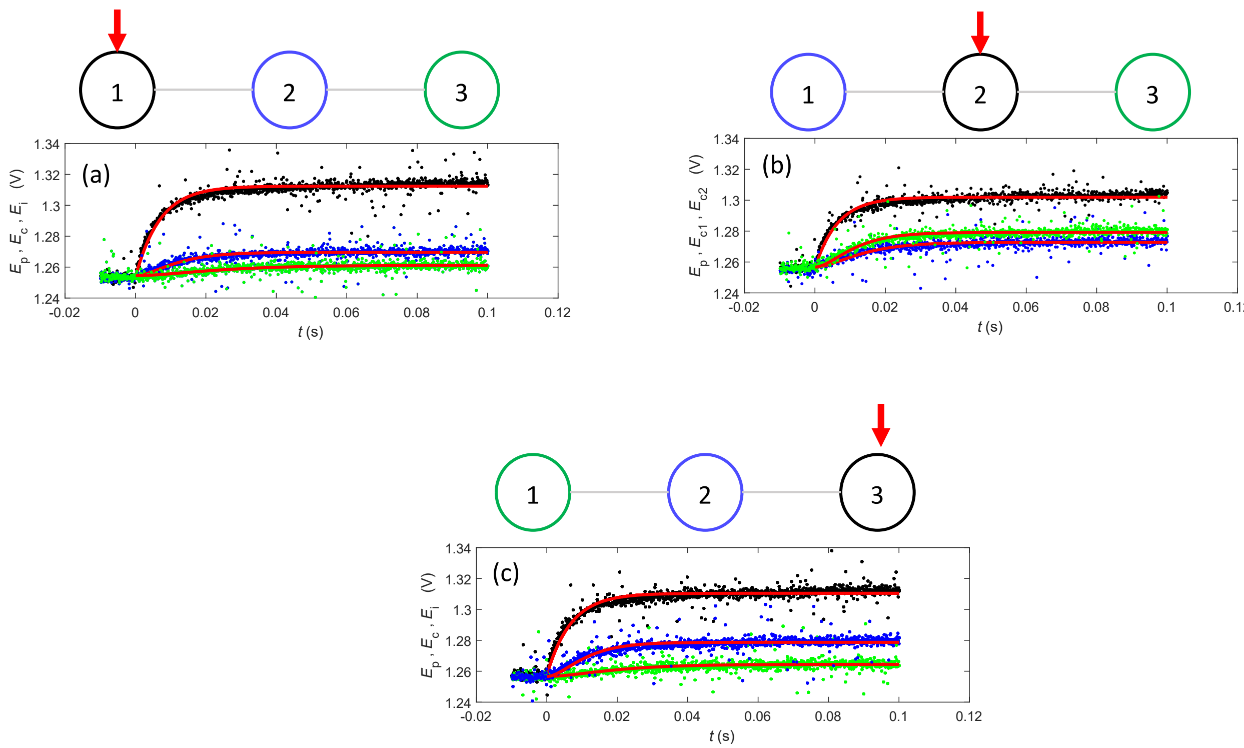

Figure 18 Inference Results for three electrodes coupled in a linear topology; (a) Perturbation of electrode 1 (b) Perturbation of electrode2 (c) Perturbation of electrode 3.

Black dotted lines represents Perturbed electrode, blue dotted lines represents directly coupled electrodes and green dotted lines represents indirectly coupled electrodes except in the case of Fig S10b where the green dotted lines also represent directly coupled electrode.

Table 6 Extracted coupling strength for three electrodes in a chain

1	Perturbed electrode 1		Perturbed electrode 2		Perturbed electrode 3	
	coupled electrode 2	coupled electrode 3	coupled electrode 1	coupled electrode 3	coupled electrode 1	coupled electrode 2
$A_1(V)$	0.059	0.059	0.046	0.046	0.053	0.053
$k_1(s^{-1})$	144.13	144.13	156.09	156.09	145.41	145.41
$A_2(V)$	0.015	0.0066	0.016	0.0022	0.0078	0.022
$k_2(s^{-1})$	155.88	76.92	136.04	163.89	93.09	168.72
$k_3(s^{-1})$	1.14	-8.14	1.12	1.73	5.73	1.53
$K_f(s^{-1})$	43.11	0.00	41.29	83.84	0.00	82.08

The ratio of the coupling strength (Φ)is given by the equation:

$$\Phi = \frac{K_{f,Y}}{K_{f,1-2}}$$

where $K_{f,Y}$ is the extracted coupling strength when electrode Y is perturbed. $K_{f,1-2}$ is the extracted coupling strength between electrode 2 and electrode 1 when electrode 2 is perturbed.

Consequently the values of the rescaled coupling strength in a three electrode arranged in a linear topology, Φ, is given in the table S7 below.

Table 7 Rescaled extracted coupling strength for three electrodes in a chain

1	Perturbed electrode 1		Perturbed electrode 2		Perturbed electrode 3	
	coupled electrode 2	coupled electrode 3	coupled electrode 1	coupled electrode 3	coupled electrode 1	coupled electrode 2
Φ	1.04	0.00	1.00	2.03	0.00	1.99

E. Complex Network

To demonstrate the accuracy of the network reconstruction technique, we applied it to a complex network containing the different types of coupling topology assessed earlier. Perturbation was applied to each individual node in the network and the evolution of the signal of the various node analyzed.

Table 8 Extracted coupling strength from perturbation of electrode 1 in a network

	Perturbed electrode 1					
	coupled electrode 2	coupled electrode 3	coupled electrode 4	coupled electrode 5	coupled electrode 6	coupled electrode 7
$A_1(V)$	0.039	0.039	0.039	0.039	0.039	0.039
$k_1(s^{-1})$	189.25	189.25	189.25	189.25	189.25	189.25
$A_2(V)$	0.021	0.015	0.0091	0.015	0.015	0.0053
$k_2(s^{-1})$	127.66	128.13	67.39	131.02	136.70	73.75
$k_3(s^{-1})$	0.48	0.94	-2.75	-2.95	-2.62	4.45
$K_f(s^{-1})$	46.23	33.28	0.00	36.47	37.85	0.00

The ratio of the coupling strength (μ)is given by the equation:

$$\mu = \frac{K_{f,Y}}{K_{f,3-1}}$$

where $K_{f,Y}$ is the extracted coupling strength when electrode Y is perturbed. $K_{f,3-1}$ is

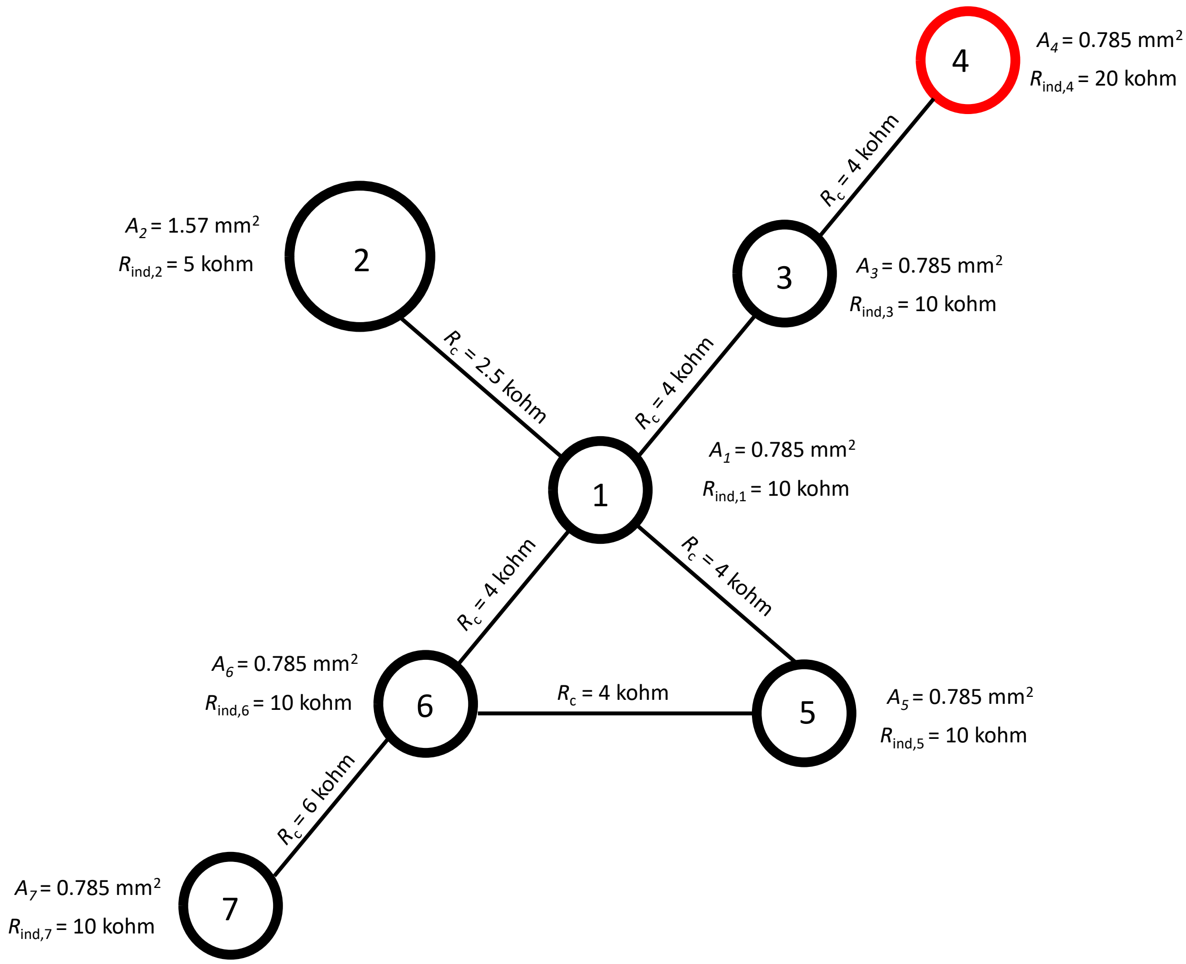

Figure 19 Complex network.

Table 9 Extracted coupling strength from perturbation of electrode 2 in a network

	Perturbed electrode 2					
	coupled electrode 1	coupled electrode 3	coupled electrode 4	coupled electrode 5	coupled electrode 6	coupled electrode 7
$A_1(V)$	0.031	0.031	0.031	0.031	0.031	0.031
$k_1(s^{-1})$	79.47	79.47	79.47	79.47	79.47	79.47
$A_2(V)$	0.010	0.0038	1.5e-04	0.0044	0.0033	0.0018
$k_2(s^{-1})$	129.71	46.44	17.09	57.07	43.09	36.88
$k_3(s^{-1})$	1.07	-354.07	-1.82e+04	-4.812	-2.1e+03	-0.39
$K_f(s^{-1})$	69.15	0.00	0.00	0.00	0.00	0.00

Table 10 Extracted coupling strength from perturbation of electrode 3 in a network

	Perturbed electrode 3					
	coupled electrode 1	coupled electrode 2	coupled electrode 4	coupled electrode 5	coupled electrode 6	coupled electrode 7
$A_1(V)$	0.031	0.031	0.031	0.031	0.031	0.031
$k_1(s^{-1})$	80.13	80.13	80.13	80.13	80.13	80.13
$A_2(V)$	0.0068	0.0014	0.018	0.0030	0.0028	0.0016
$k_2(s^{-1})$	112.20	30.63	76.08	45.75	73.38	42.11
$k_3(s^{-1})$	1.19	-0.007	0.063	-0.0019	-1.42	-5.99
$K_f(s^{-1})$	33.77	0.00	41.86	0.00	0.00	0.00

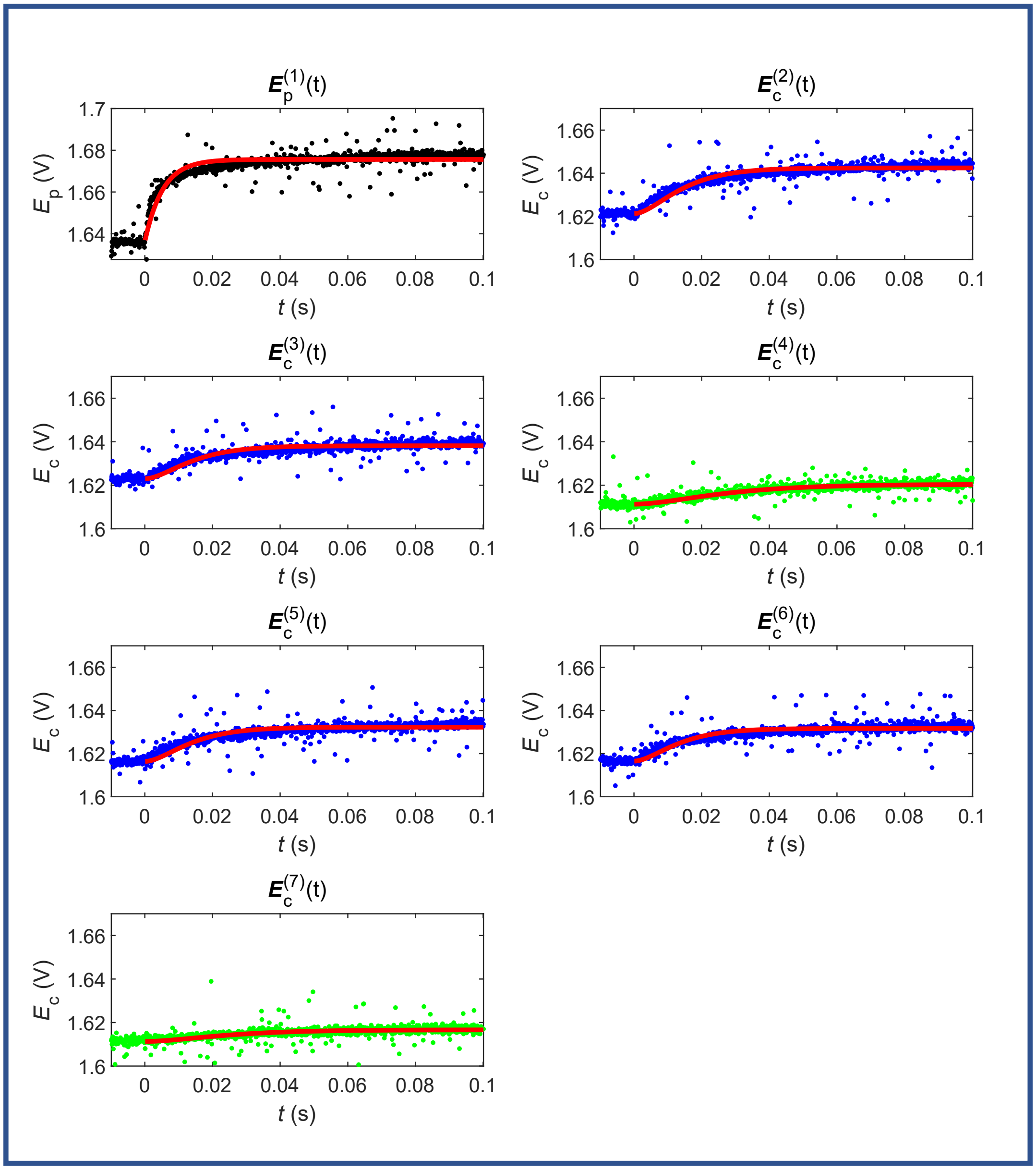

Figure 20 Inference Results for complex network; Perturbation of electrode 1. Black dotted lines represents Perturbed electrode, blue dotted lines represents directly coupled electrodes and green dotted lines represents indirectly coupled electrodes

the extracted coupling strength between electrode 1 and electrode 3 when electrode 1 is perturbed. Consequently the values of the rescaled coupling strength in a complex network, μ, is given in the table S16 below

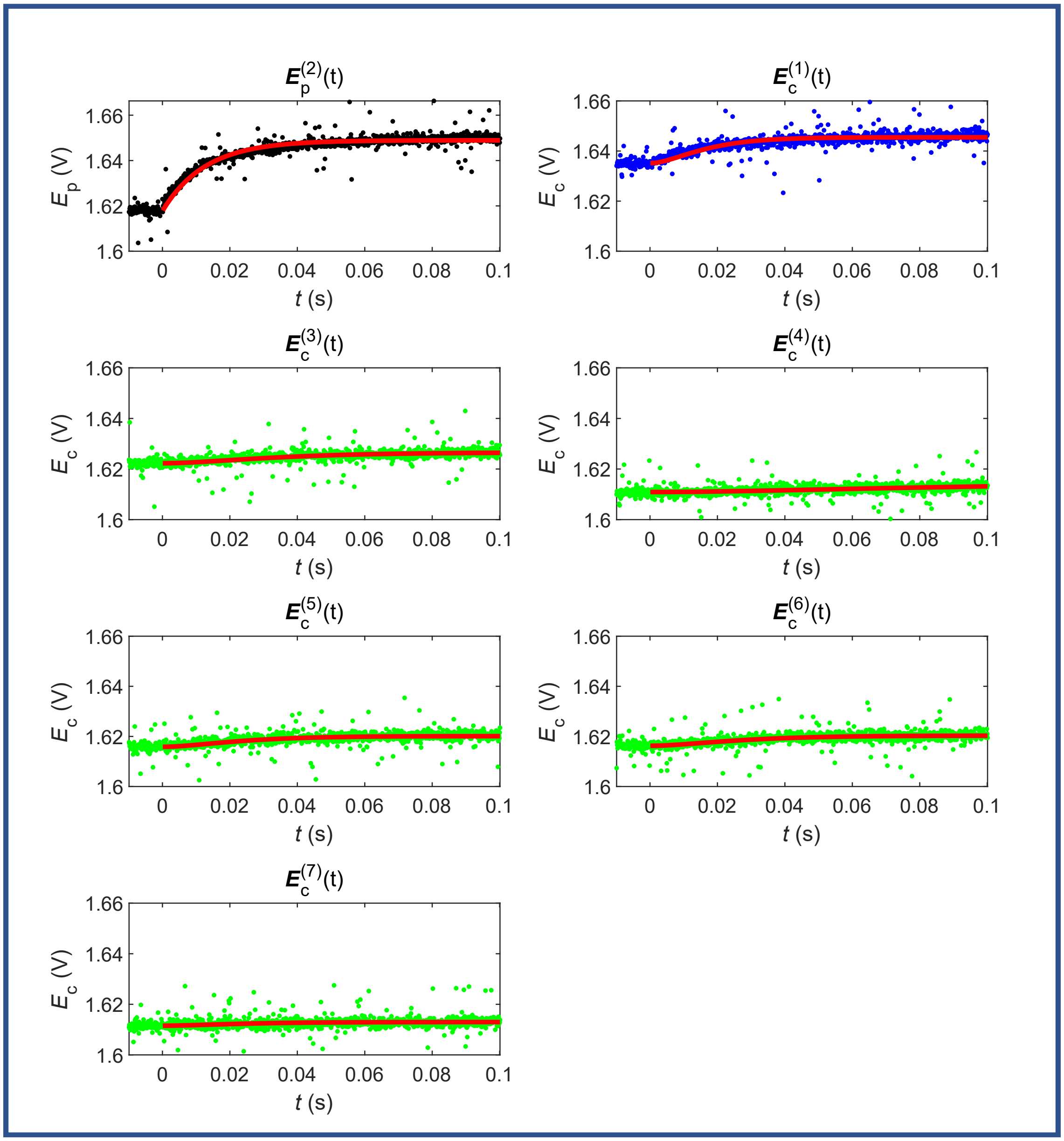

Figure 21 Inference Results for complex network; Perturbation of electrode 2. Black dotted lines represents Perturbed electrode, blue dotted lines represents directly coupled electrodes and green dotted lines represents indirectly coupled electrodes

Table 11 Extracted coupling strength from perturbation of electrode 4 in a network

Perturbed electrode 4						
	coupled electrode 1	coupled electrode 2	coupled electrode 3	coupled electrode 5	coupled electrode 6	coupled electrode 7
$A_1(V)$	0.027	0.027	0.027	0.027	0.027	0.027
$k_1(s^{-1})$	61.53	61.53	61.53	61.53	61.53	61.53
$A_2(V)$	0.0023	0.0005	0.0092	0.0009	0.00002	0.0002
$k_2(s^{-1})$	77.87	13.46	84.23	57.19	23.43	55.73
$k_3(s^{-1})$	-8.33	-985.30	1.60	-6.39	-0.0006	-0.0002
$K_f(s^{-1})$	0.00	0.00	38.27	0.00	0.00	0.00

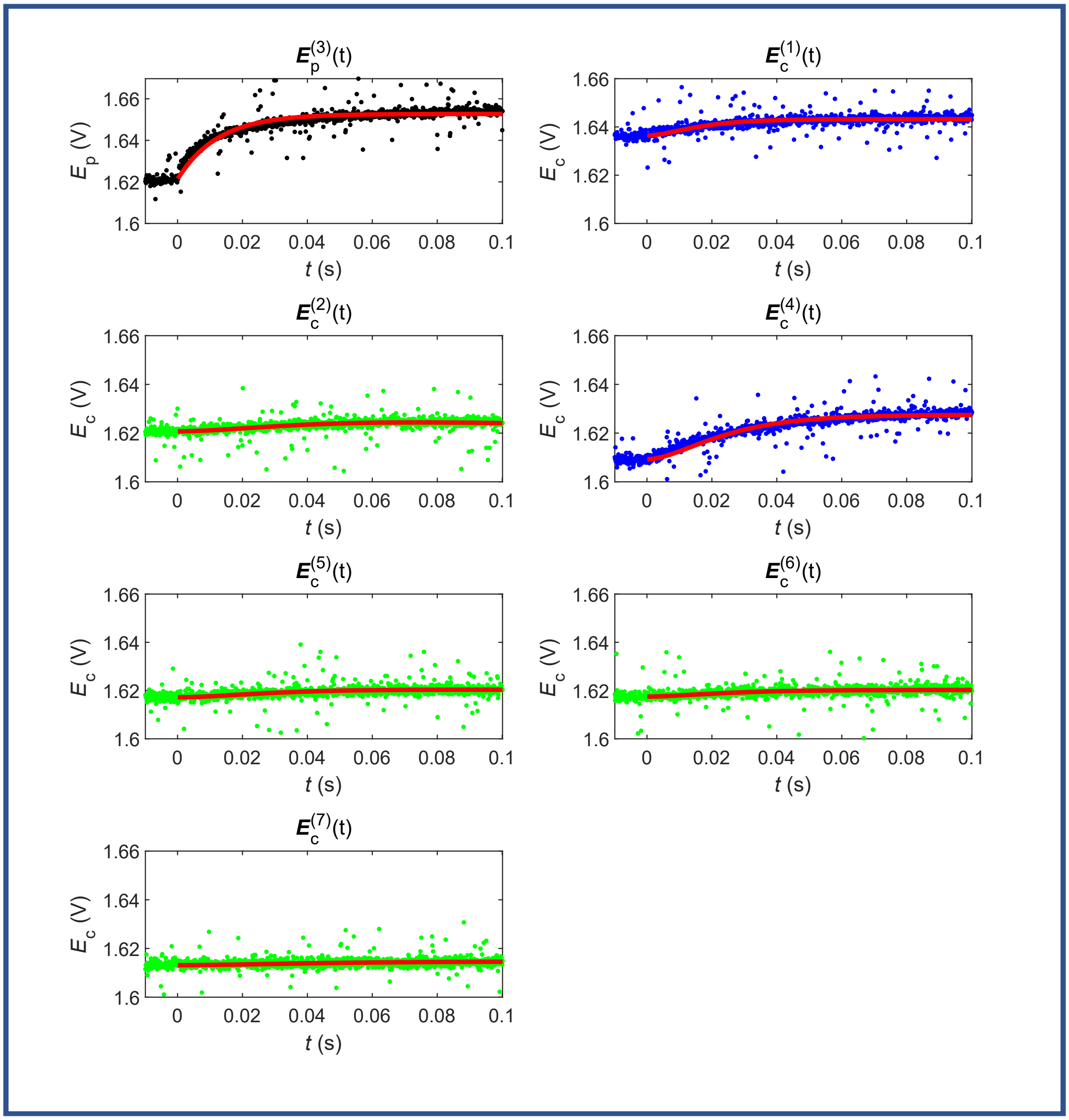

Figure 22 Inference Results for complex network; Perturbation of electrode 3. Black dotted lines represents Perturbed electrode, blue dotted lines represents directly coupled electrodes and green dotted lines represents indirectly coupled electrodes

Table 12 Extracted coupling strength from perturbation of electrode 5 in a network

	Perturbed electrode 5					
	coupled electrode 1	coupled electrode 2	coupled electrode 3	coupled electrode 4	coupled electrode 6	coupled electrode 7
$A_1(V)$	0.027	0.027	0.027	0.027	0.027	0.027
$k_1(s^{-1})$	103.13	103.13	103.13	103.13	103.13	103.13
$A_2(V)$	0.0078	0.0042	0.0026	0.0012	0.0093	0.0030
$k_2(s^{-1})$	113.88	69.29	54.59	0.052	107.37	60.00
$k_3(s^{-1})$	0.39	-3.86	-2.59	249.37	1.17	9.79
$K_f(s^{-1})$	35.50	0.00	0.00	0.00	37.86	0.00

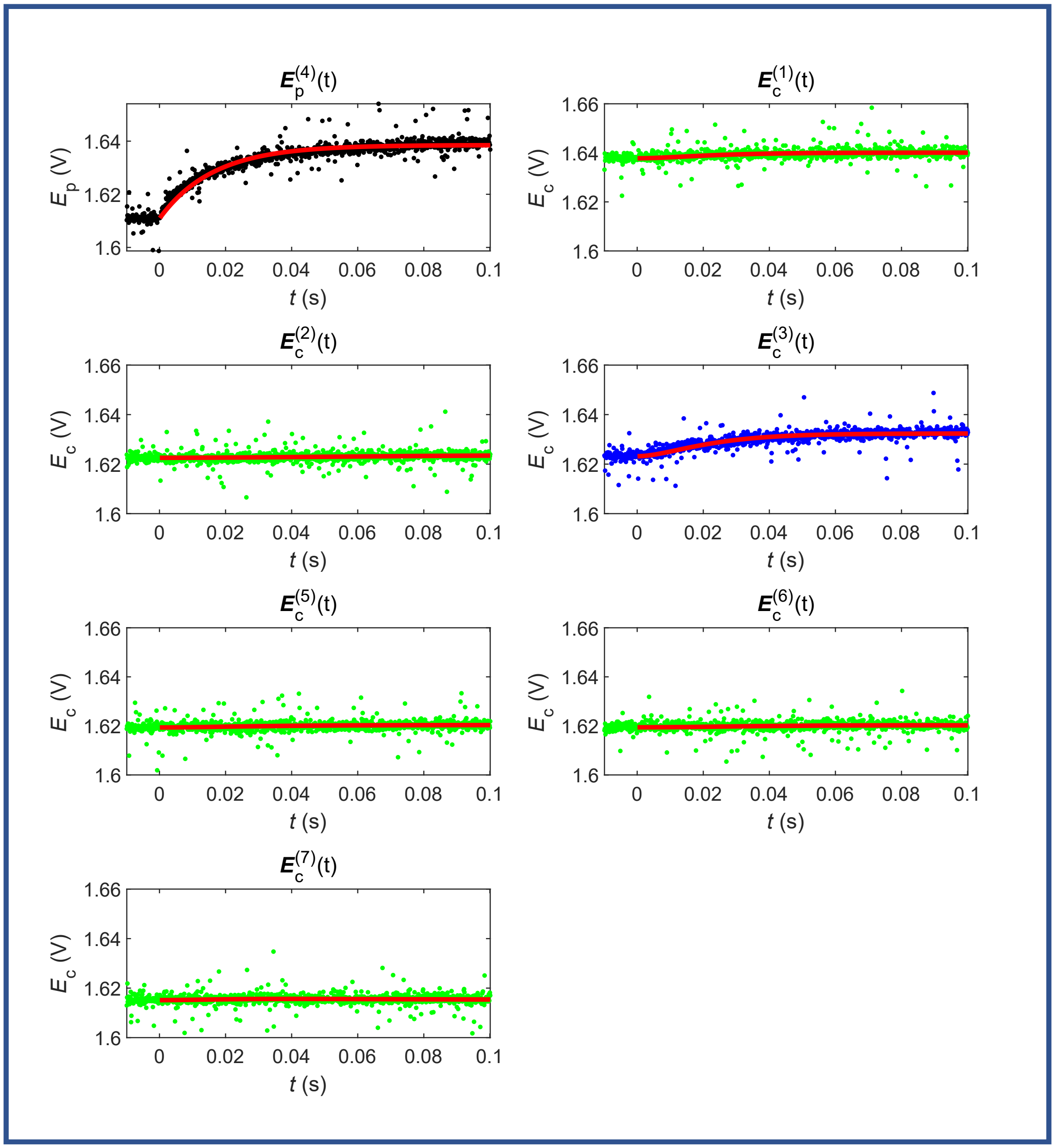

Figure 23 Inference Results for complex network; Perturbation of electrode 4. Black dotted lines represents Perturbed electrode, blue dotted lines represents directly coupled electrodes and green dotted lines represents indirectly coupled electrodes

Table 13 Extracted coupling strength from perturbation of electrode 6 in a network

	Perturbed electrode 6					
	coupled electrode 1	coupled electrode 2	coupled electrode 3	coupled electrode 4	coupled electrode 5	coupled electrode 7
$A_1(V)$	0.024	0.024	0.024	0.024	0.024	0.024
$k_1(s^{-1})$	108.75	108.75	108.75	108.75	108.75	108.75
$A_2(V)$	0.0074	0.0035	0.0013	0.0013	0.0096	0.0083
$k_2(s^{-1})$	119.05	76.99	61.26	51.73	97.48	80.17
$k_3(s^{-1})$	2.22	8.21	5.91	-9.54	0.64	1.09
$K_f(s^{-1})$	39.49	0.00	0.00	0.00	34.63	20.25

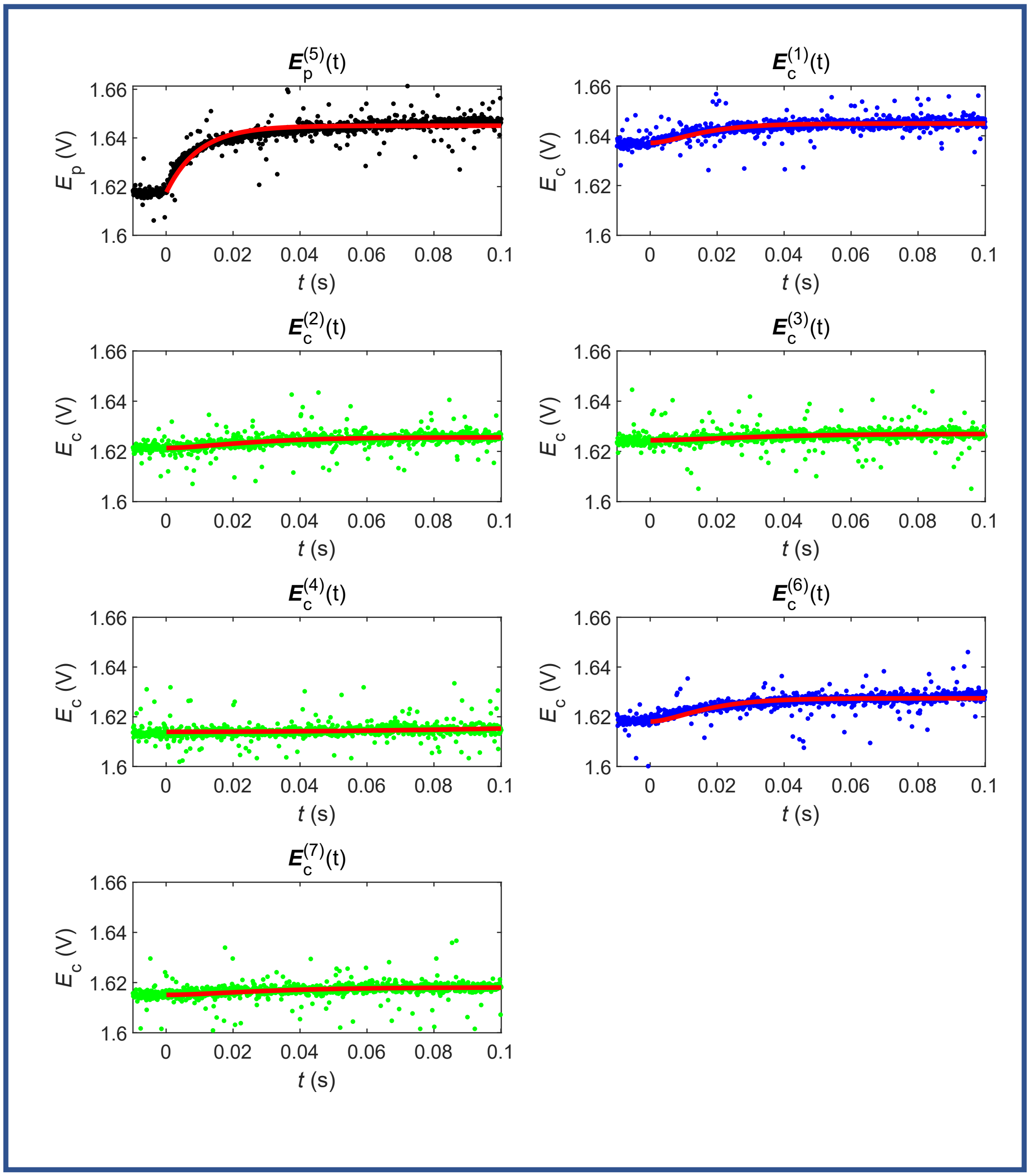

Figure 24 Inference Results for complex network; Perturbation of electrode 5. Black dotted lines represents Perturbed electrode, blue dotted lines represents directly coupled electrodes and green dotted lines represents indirectly coupled electrodes

Table 14 Extracted coupling strength from perturbation of electrode 7 in a network

	Perturbed electrode 7					
	coupled electrode 1	coupled electrode 2	coupled electrode 3	coupled electrode 4	coupled electrode 5	coupled electrode 6
$A_1(V)$	0.041	0.041	0.041	0.041	0.041	0.041
$k_1(s^{-1})$	74.64	74.64	74.64	74.64	74.64	74.64
$A_2(V)$	0.0021	0.00008	0.0011	2e-06	0.0028	0.0078
$k_2(s^{-1})$	55.05	2.47	8.47	-33.42	59.39	87.58
$k_3(s^{-1})$	3.98	5.82	-325.4	-0.0023	-1.38	-1.79
$K_f(s^{-1})$	0.00	0.00	0.00	0.00	0.00	19.55

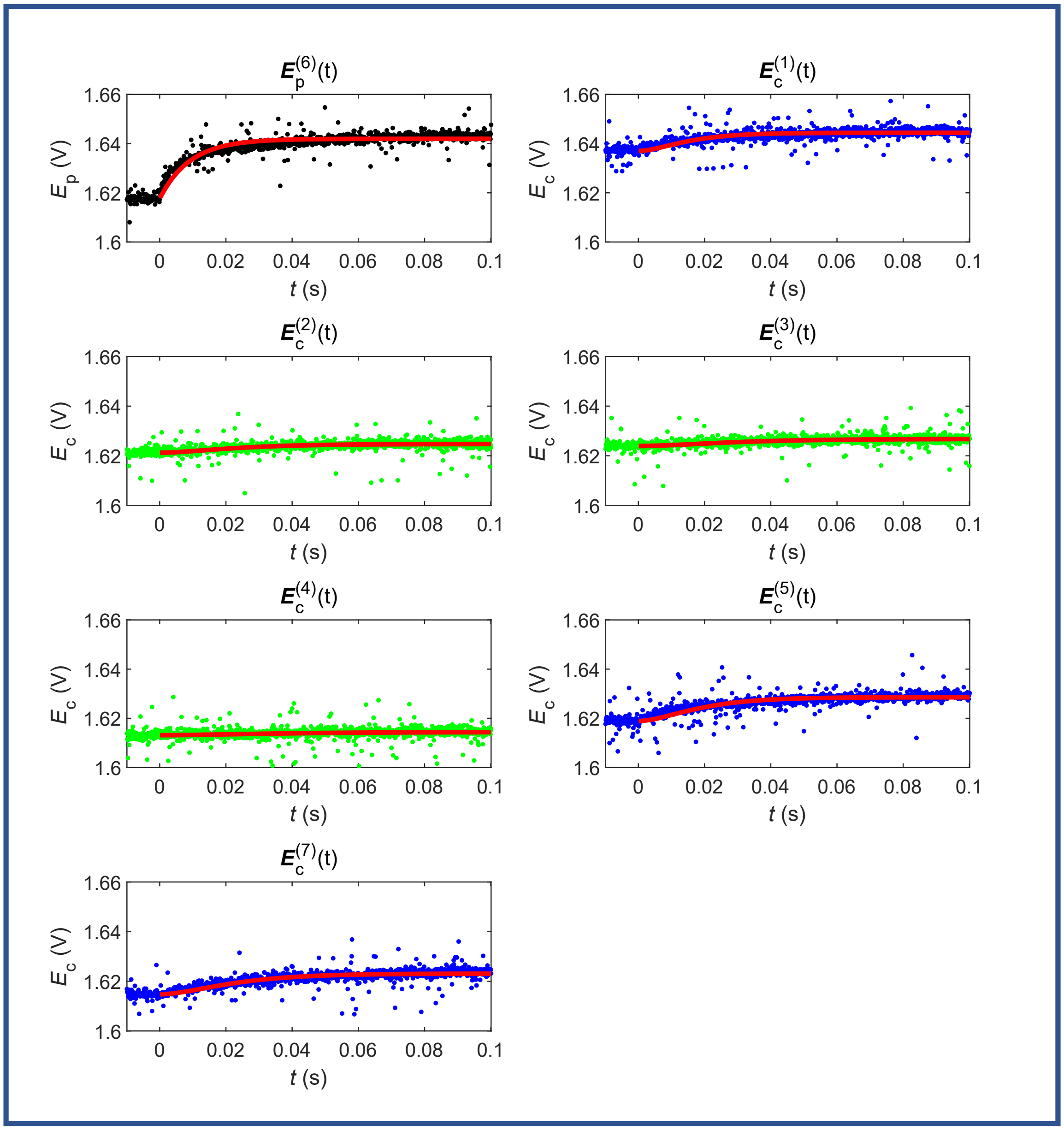

Figure 25 Inference Results for complex network; Perturbation of electrode 6. Black dotted lines represents Perturbed electrode, blue dotted lines represents directly coupled electrodes and green dotted lines represents indirectly coupled electrodes

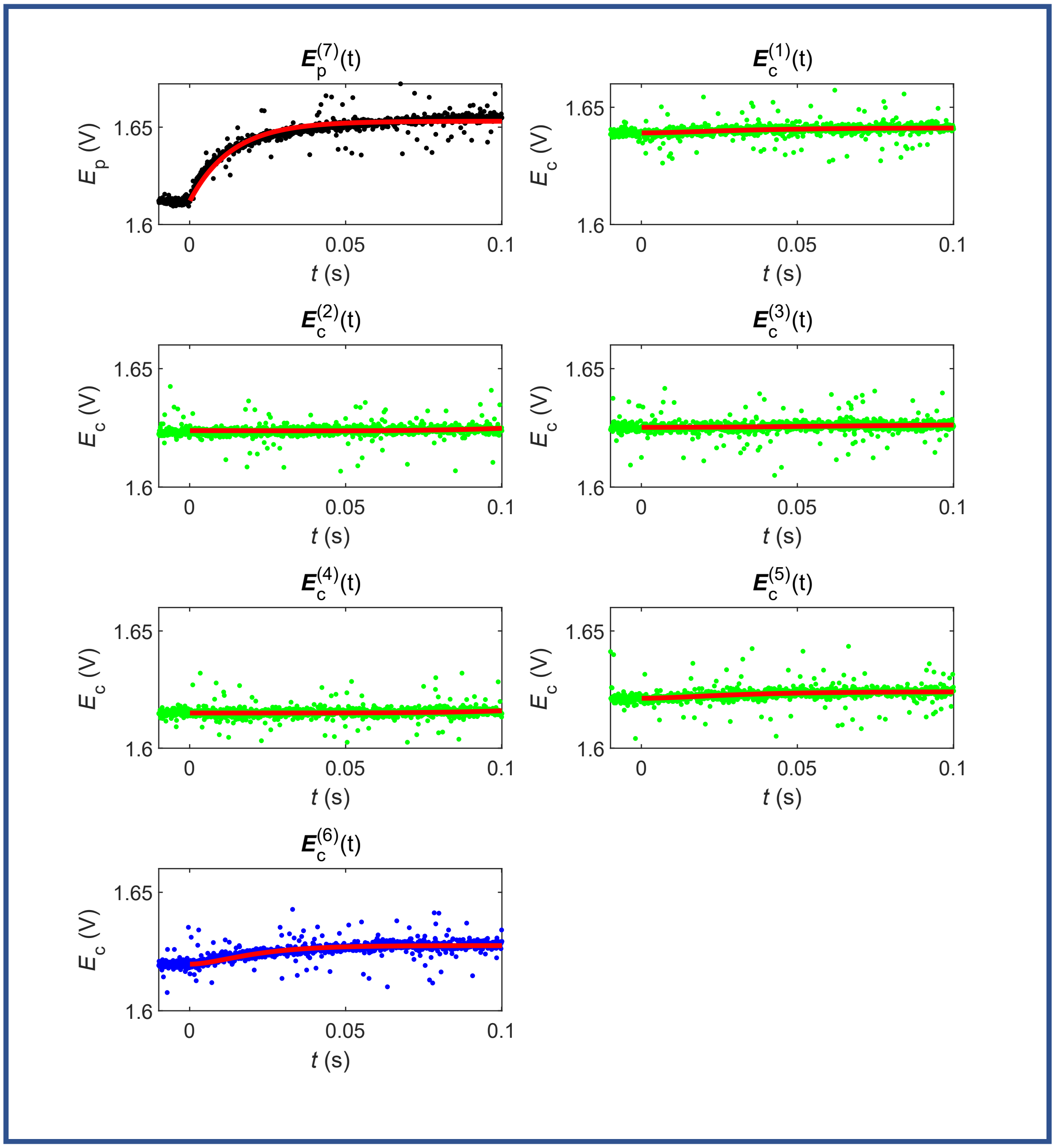

Figure 26 Inference Results for complex network; Perturbation of electrode 7. Black dotted lines represents Perturbed electrode, blue dotted lines represents directly coupled electrodes and green dotted lines represents indirectly coupled electrodes

Table 15 Extracted coupling strengths from the network topology

Perturbed electrode 1						
	coupled electrode 2	coupled electrode 3	coupled electrode 4	coupled electrode 5	coupled electrode 6	coupled electrode 7
$K_f(s^{-1})$	46.23	33.28	0.00	36.47	37.85	0.00
Perturbed electrode 2						
	coupled electrode 1	coupled electrode 3	coupled electrode 4	coupled electrode 5	coupled electrode 6	coupled electrode 7
$K_f(s^{-1})$	69.15	0.00	0.00	0.00	0.00	0.00
Perturbed electrode 3						
	coupled electrode 1	coupled electrode 2	coupled electrode 4	coupled electrode 5	coupled electrode 6	coupled electrode 7
$K_f(s^{-1})$	33.77	0.00	41.86	0.00	0.00	0.00
Perturbed electrode 4						
	coupled electrode 1	coupled electrode 2	coupled electrode 3	coupled electrode 5	coupled electrode 6	coupled electrode 7
$K_f(s^{-1})$	0.00	0.00	38.27	0.00	0.00	0.00
Perturbed electrode 5						
	coupled electrode 1	coupled electrode 2	coupled electrode 3	coupled electrode 4	coupled electrode 6	coupled electrode 7
$K_f(s^{-1})$	35.50	0.00	0.00	0.00	37.86	0.00
Perturbed electrode 6						
	coupled electrode 1	coupled electrode 2	coupled electrode 3	coupled electrode 4	coupled electrode 5	coupled electrode 7
$K_f(s^{-1})$	39.49	0.00	0.00	0.00	34.63	20.25
Perturbed electrode 7						
	coupled electrode 1	coupled electrode 2	coupled electrode 3	coupled electrode 4	coupled electrode 5	coupled electrode 6
$K_f(s^{-1})$	0.00	0.00	0.00	0.00	0.00	19.55

Table 16 Rescaled extracted coupling strengths from the network topology

Perturbed electrode 1						
	coupled electrode 2	coupled electrode 3	coupled electrode 4	coupled electrode 5	coupled electrode 6	coupled electrode 7
μ	1.38	1.00	0.00	1.09	1.13	0.00
Perturbed electrode 2						
	coupled electrode 1	coupled electrode 3	coupled electrode 4	coupled electrode 5	coupled electrode 6	coupled electrode 7
μ	2.10	0.00	0.00	0.00	0.00	0.00
Perturbed electrode 3						
	coupled electrode 1	coupled electrode 2	coupled electrode 4	coupled electrode 5	coupled electrode 6	coupled electrode 7
μ	1.01	0.00	1.25	0.00	0.00	0.00
Perturbed electrode 4						
	coupled electrode 1	coupled electrode 2	coupled electrode 3	coupled electrode 5	coupled electrode 6	coupled electrode 7
μ	0.00	0.00	1.15	0.00	0.00	0.00
Perturbed electrode 5						
	coupled electrode 1	coupled electrode 2	coupled electrode 3	coupled electrode 4	coupled electrode 6	coupled electrode 7
μ	1.06	0.00	0.00	0.00	1.14	0.00
Perturbed electrode 6						
	coupled electrode 1	coupled electrode 2	coupled electrode 3	coupled electrode 4	coupled electrode 5	coupled electrode 7
μ	1.18	0.00	0.00	0.00	1.04	0.60
Perturbed electrode 7						
	coupled electrode 1	coupled electrode 2	coupled electrode 3	coupled electrode 4	coupled electrode 5	coupled electrode 6
μ	0.00	0.00	0.00	0.00	0.00	0.60